Deliverable D7.1

Definition of methodology for the system evaluation of SPRINTER technology

Lead Beneficiary	**TEI**
Contact Person	Alfredo Palagi
Address	Via E. Melen, 77 – 16152 Genova (Italy)
Phone	+393351258202
e-mail	alfredo.palagi@ericsson.com

Date due of deliverable	31.12.2023 [M16]
Actual submission date	27.02.2024 [M18]
Authors	|TEI A. Palagi, G. Sacco |ICCS E. Andrianopoulos, G. Megas, P. Basaras, N.K. Lyras |NVIDIA D. Syrivelis, N. Argyris |ICOM E. Pikasis, D. Kritharidis |CMC Saimanoj Katta, Jose Costa-Requena, |FILL L. Probst, H. Sehrschön
Participants	TEI, ICCS, NVIDIA, UC3M, ICOM, CMC, FILL

Work-package	WP7
Dissemination level	PU
Type	Report
Version	1.0
Total number of pages	50

SPRINTER | HORIZON-IA
HORIZON-CL4-2021-DIGITAL-EMERGING-01-06
Project no.: 101070581
Start Date: 1 September 2022
Duration: 42 Months

Document History

Version	Date dd.mm.yy	From > To	Description
V02	29.11.2023	ICOM > ICCS	Input for Module-4 Rx testing
V03	30.11.2023	ICCS > TEI	Section 2
V04	13.12.2023	ICCS>TEI	Section 3.2
V05	18.01.2024	TEI > All	All section completed; Ready for internal review
V06	09.02.2024	TEI > All	Updates on Chapter 3
V07	13.02.2024	TEI > All	General review of the document
V0.8	27/02/2024	TEI > All	Final version
V1.0	27/02/2024	PC>EU	Submission

List of abbreviations

3G/4G/5G /6G	Second/third/fourth/fifth generation mobile communication networks
3GPP	Third Generation Partnership Project
5GC	5G Core
AAS	Advanced Antenna System
AIR	Antenna Integrated Radio
ADC	Analogue to Digital Converter
AI	Artificial Intelligence
API	Application Programming Interface
AWG	Arbitrary Waveform Generator
BB	Base Band
BBU	Base Band Unit
BER	Bit error rate
BPF	Band Pass Filter
BPP	Bits per Pixel
C2	Command and Control
cAWG	cyclic Arrayed Waveguide Gratings
CA	Consortium Agreement
CNC	Centralized Network Controller
COTS	Commercial Off The Shelf
CP	Control Plane
CPRI/eCPRI	Common Public Radio Interface/enhanced CPRI
CPU	Central Processing Unit
CRI	Carrier Re-Insertion
CTLE	Continuous Time Linear Equalization
CW	Continuous Wave
dB	Decibel
dBi	Decibels with respect to an isotropic antenna reference
EAM	Electro-Absorption Modulator
EE	End Effector
DAC	Digital to Analogue Converter
DAC	Direct Attached Cable
DC	Direct Current
DFB	Distributed FeedBack
DMZ	Demilitarized Zone
DL	Downlink
DU	Distributed unit
E2E	End to End
ECL	External Cavity Laser
EDFA	Erbium Doped Fiber Amplifier
EE	end-effector
EIRP	Equivalent Isotropic Radiated Power
EOM	Electro-Optical Modulator
ER	Extinction Ratio
eMBB	Enhanced Mobile Broadband
eNB	Enhanced Node B (4G base station)
ESA	Electrical Spectrum Analyzer
EU	European Union

FH	Fronthaul
FN	Fixed Node
FPS	Frames Per Second
FSO	Free Space Optical
GaAs	Gallium Arsenide
GB	Gigabyte
Gbps	Gigabits per second
GDP	Gross domestic product
GHz	Gigahertz
gPTP	Generic Precision time Protocol
KPI	Key Performance Indicator
IMT	International Mobile Telecommunications
IF	Intermediate Frequency
IIoT	Industrial Internet of Things
InP	Indium Phosphide
ITU	International Telecommunications Union
LCM	LifeCycle Management
LD	Laser Diode
LNOI	Lithium Niobate On Insulator
LO	Local Oscillator
LOS	Line of Sight
MANO	MANagement and Orchestration
MCF	Multicore Fiber
MEC	Mobile Edge Computing
MH	Midhaul
MHz	Megahertz
MIMO	Multiple Input Multiple Output
mMIMO	massive MIMO
MMI	Multi-Mode Interference
MP	Mega Pixel
MPO	Multi-fiber Push On
mMTC	Massive Machine Type Communications
mmWave	Millimeter Wave
MN	Mobile Node
MZI	Mach-Zehnder Interferometer
MZM	Mach-Zehnder Modulator
MW	Microwave
NC	Numerical Control
NCU	Numerical Control Unit
NTC	Negative Temperature Coefficient
NFV	Network Function Virtualization
NETCONF	Network Configuration Protocol
NIC	Network Interface Card
NLOS	Non-Line of Sight
NR	New Radio
NRZ	Non-Return to Zero
NSA/SA	Non-Standalone / Standalone (5G implementation options)
OAI	Open Air Interface

OBFN	Optical Beam-Forming Network
OFCG	Optical Frequency Comb Generator
OOK	On Off Keying
OMA	Optical Modulation Amplitude
OSA	Optical Spectrum Analyzer
OTT	Over the Top
ORAN	Open RAN
PCA	Photoconductive Antenna
PCIe	Peripheral Component Interconnect Express
PD	Photo Diode
PDL	Polarization Dependent Loss
PIC	Photonic Integrated Circuit
PLC	Programmable Logic Computer
PLO	Phased Lock Oscillator
PM	Phase Modulator
PoP	Point of Presence
PTP	Precision Time Protocol
PZT	Depositing lead zirconate titanite
QoS	Quality of Service
QSFP	Quad Small Form-factor Pluggable
RAN	Radio Access Network
RAT	Radio Access Technology
REST	REpresentational State Interface
RIN	Relative Intensity Noise
RF	Radio Frequency
RN	Remote Node
ROADM	Reconfigurable Optical Add-drop Multiplexer
RSOA	Reflective Semiconductor Optical Amplifier
RRH	Radio Remote Head
RTO	Real Time Oscilloscope
SDN	Software Defined Network
SDO	Standard Developing Organization
SDR	Software Defined Radio
SFP	Small Form-factor Pluggable
SM	Single Mode
SMF	Single Mode Fiber
SNR	Signal to Noise Ratio
SOA	Semiconductor Optical Amplifier
srsLTE	Software Radio Systems LTE implementation (open source)
TCP	Tool – Centre Point
TDEC	Transmission and Dispersion Eye Closure
TDD	Time Division Duplex
TEC	Thermo-Electrical Cooler
THz	Terahertz
TIA	Transimpedance Amplifier
TL	Tunable Laser
TRx	Transceiver
TSN	Time Sensitive Networking

TT	TSN Translation
UE	User Equipment
UHD	Ultra-High Definition
UP	User Plane
UL	Uplink
uRLLC	Ultra-Reliable Low Latency Communications
VCSEL	Vertical-Cavity Surface-Emitting Laser
vEPC	Virtual Evolved Packet Core
VNA	Vector Network Analyzer
VOA	Variable Optical Attenuator
VPN	Virtual Private Network
VR/AR/xR	Virtual Reality / Augmented Reality *(Note: xR applies to both)*
WPx	Work Package #x
WPAN	Wireless Personal Area Network

Executive Summary

SPRINTER aims to develop a set of low-cost, energy-efficient, and ultra-dynamic optical transceivers optical switching solutions to cope with the diverse needs of the industrial networks and expedite their truly digital transformation. In order to showcase SPRINTER's full potential, the developed technology will be evaluated within application scenarios that will be deployed in a relevant industrial environment incorporating a fully operational closed-loop control system.
Aim of this deliverable is to describe the different phases of testing that will assess the adherence of SPRINTER prototypes to component and network KPIs.
To fully exploit SPRINTER modules performances, three levels of test were identified: module level testing, system level testing and industrial application testing.
After a first chapter that introduces purpose and structure of the document, the three subsequent chapters (two, three and four) are dedicated to the description of each test phase while last chapter draws the conclusions of SPRINTER framework definition for the system characterization and evaluation.
For each of the identified test phase is described location (lab or industrial premise) of the activity, the partner that will take care of it, the setup that will be used, the instruments and tools required and the relevant parameters and KPIs that will be possible to assess at that test step.

Final goal is to be able to cover all the relevant KPIs for optical components designed for industrial network application that were described in **D2.1**[1].

On **Chapter 2** module level test strategy of **Module 1a/b**, **Module 2a/b**, **Module 3** and **Module 4 FN/RN,** are described by **ICCS** that is responsible of module level testing of optical components in their lab.

Chapter 3 contains the description of three system level tests:
- NVIDIA NICs and **CMC Centralized Network Controller** integration and verification in **CMC** premises;
- **Module 1a/b**, **Module 3** and **network components** in fronthaul connectivity of **TEI** end-to-end 5G RAN network;
- **Module 2a/b**, **Module 4 FN/RN** and **network components** in **ICCS** testbed.

Within **Chapter 4 FILL** describes the industrial network application of SPRINTER architecture and innovative components to enable connectivity for industrial robot control through analysis of high-resolution videos.

Keywords: Industrial communication, industrial communication network, use case, application scenarios, optical communications, Industry 4.0, KPI, AI, process automation, quality assurance, cobots, mmWave, FSO, local machine cell, integration, testing, test strategy.

1 INTRODUCTION

1.1 Purpose of this document

D7.1 - Definition of methodology for the system evaluation of SPRINTER technology document is intended to use benchmarks defined in D2.1[1] of the same project to define the overall test strategy of SPRINTER HW and SW components.

SPRINTER deliverables are a set of innovative optical components (Fibre optical and hybrid FSO/mmWave Transceivers and Optical switches) that make possible to deploy TSN network in Industry 4.0 factory.

At very high-level test strategy defined in SPRINTER project requires that each HW and SW component of the target network architecture shall be firstly verified individually, secondly experimentally evaluated together with others at subsystem level and then deployed in the target Industry 4.0 environment in FILL premises for the overall end to end validation.

The aim of this document is to describe the three phases of SPRINTER HW and SW deliverables validation process and the KPIs used during each test phase to assess results; this document is also describing the test setups, their locations and the test activity owners.

1.2 Document structure

Present document is organized in three main chapters plus introduction and conclusion ones.

Each of the three main chapters contains description of the test activities foreseen for one validation phase:

- Chapter 2
  Module level evaluation
  Description of different test phases for Module 1 (a and b variants), Module 2 (a and b variants), Module 3 and Module 4 (RN and FN variants), that include static measures and dynamic ones. For each of the test phase reference KPI for the module validation are indicated.
- Chapter 3
  System integration and validation
  Three subsystems were identified in accordance with SPRINTER architecture for the system integration and validation phase: Network component for TSN network (tested by CMC), TSN backbone optical connectivity (comprising Module 1 and 3, tested in RAN E2E setup by TEI), and Local cell optical connectivity (comprising Module 2 and 4, tested by ICCS). For each of the test phase reference KPI for the module validation are indicated.
- Chapter 4
  Industrial premises field trial
  The SPRINTER technology is validated in relevant industrial production, represented by the environment at Fill premises. The demonstration is linked to applications in shopfloor control-systems, based on standard industrial level.

1.3 Audience

This deliverable is a public report; it represents the output of SPRINTER *T7.1 - Definition of testing procedures and demonstration scenarios* and forms the basis for the work to be carried out in the rest of the work package *WP7 – System integration and testing of SPRINTER prototypes* by all partners inside SPRINTER consortium.

2 MODULE LEVEL EVALUATION

In this chapter, the methodologies to be implemented during the benchtop tests of the modules in the lab of ICCS/NTUA are described. These tests aim to validate their basic operation and intended functions. Under this context, ICCS will leverage the monitoring ports that are available in all SPRINTER prototypes through the fiber array, to evaluate each component of the modules separately and validate its base-line operation. Considering that SPRINTER prototypes use the same set of optical components, most of the testing procedures that will be followed are common within the prototypes. These include static optical (light current voltage (LIV) curves, optical power, etc) and electrical (e.g., current voltage (IV) curves, S-parameters, DC/RF) measurements of each tuning and active photonic element, and electrical components as well as the system evaluation and characterization of all units/parts of the Modules. Considering the sensitivity of these components, special care should be given to ensuring that the testing processes do not harm the module. To that end, translation boards will be used, using ribbon cables to connect to the DC connector hosted on the chip's PCB. Using jumper cables and a high-precision multimeter, each heater and active element is tested separately in order to verify whether the specific component is functional, and the observed measurement matches the expected value (ohmic resistance or diode forward voltage), or if there is an issue with the specific component, in which case a visual inspection follows as a debugging step, to try and identify the issue. Specifically for the active elements, IV measurements should also be performed for a range of input voltages to ensure they exhibit the expected performance. Visual inspection is performed by means of microscopes, to identify possible issues on the wire-bonding parts, the routing on each photonic platform and on the PCB, etc. Finally, characterization regarding the coupling losses between the platforms should take place leveraging the alignment loops that are accommodated on the Modules, via the fiber array. In parallel, the electronic control units which will be developed for the operation of each Module will also be tested, and their performance will be assessed before the integration of the Modules with the control units. To that end, in a similar rationale as discussed above, translation circuits are employed using testing resistances to make sure that the current and voltage sources provide the correct value, characterizing the performance in terms of time stability, and response to radical changes (identification of possible spikes that could harm the optical chip). As a final step the control electronic units will be integrated with the respective modules and the benchtop testing of all the units of each Module will be performed as decided in the following subsections.

Figure 1: Indicative schematic representation of the "static" measurements' experimental setup. (a) Electrical (b) Optical

2.1 Module 1 test strategy

SPRINTER aims on the development of 200 Gb/s transceivers based on two different, powerful design concepts targeting low power consumption, and low fabrication and assembly cost. These two concepts comprise the two different versions of SPRINTER's Module 1, taking advantage of hybrid photonic integration techniques having a polymer-based photonic platform named PolyBoard as the PICs' motherboard. Specifically, Module-1a is based on 4-fold InP Electro-absorption Modulated Laser (EML) arrays operating in the O-band at its transmitter side, targeting 50 Gb/s NRZ OOK transmission at distances of up to 2 km, whereas at its receiver side is based on 4-fold InP based photodiodes (PDs), capable of detecting and down-converting the 50 Gb/s optically modulated signals. On the other hand, Module-1b comprises 4-fold single-mode GaAs VCSEL arrays operating at the 1060 nm regime as its main building blocks, targeting identical modulation parameters, for transmission distances up to 500 m, with 4-fold InP-based PD arrays at its receiver. During the testing campaigns of the packaged Module-1 prototypes, a step-wise approach will be followed which will be described in detail in the next subsections, starting with the evaluation of each individual component at the transmitter and receiver side of both versions of Module-1 employing external testing equipment, followed by the evaluation of the performance of the prototype as a whole, finally leading to its integration into a systemic experimental setup, determining and evaluating the key performance indicators (KPIs) within each one of these phases.

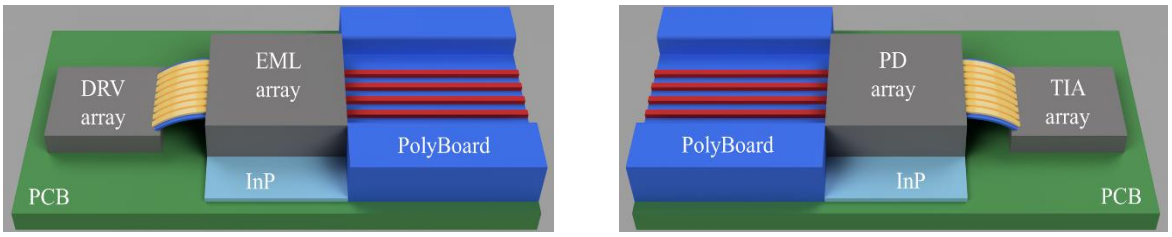

(a) (b)

Figure 2: Artistic layouts of the Module-1a EML-based O-band a) transmitter and b) receiver.

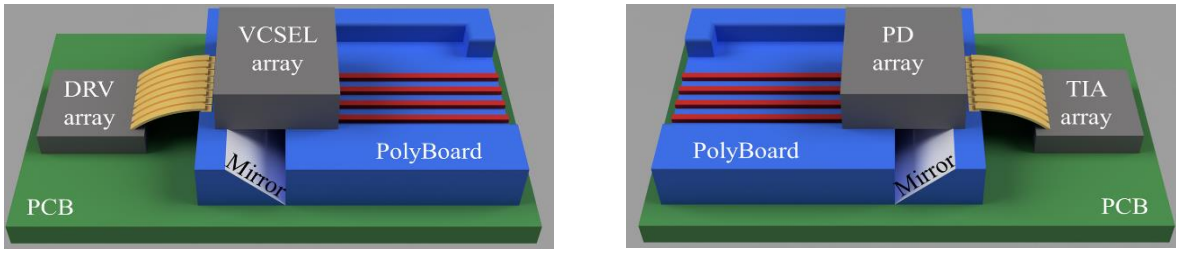

(a) (b)

Figure 3: Artistic layouts of the Module-1b VCSEL-based 1060nm regime a) transmitter and b) receiver.

2.1.1 Module 1a lab test

Static Measurements

The testing of the packaged prototypes initiates with the so-called "static" electrical and optical measurements to firstly verify the proper packaging of the module and that the interconnection between the electrical and optical parts of the prototypes is solid and has not suffered any damage e.g., during the prototype's shipping. These "static" measurements in the optical domain consist of measuring the coupling losses between the different photonic platforms that each module consists of. This measurement is facilitated by the fiber array that the prototypes host where, during the design

phase of the prototype, corresponding ports have been included to create loops in the photonic platforms allowing us to assess solely the coupling losses, without propagating through any passive or active optical component but rather through simple circular waveguides. The electrical "static" measurements are facilitated by the use of a multimeter, carefully selected to make sure that its built-in characteristics do not pose any dangers to the sensitive optical components. Then, through the use of passive PCB interposers or simple cables, each optical component is measured through either ohmic or diode measurements from the multimeter to firstly verify that the wirebonds responsible for interconnecting the PCB to the optical chip have not suffered any damage, as well as make sure that the values regarding e.g., the ohmic resistance (measured mostly for the passive optical components) and the diode voltage drop (measured mostly for the active optical components) are indeed the expected ones. These tests serve as the first step towards evaluating each prototype, giving us a solid first idea on the existence of possible issues towards the testing of the individual optical units as well as the system tests.

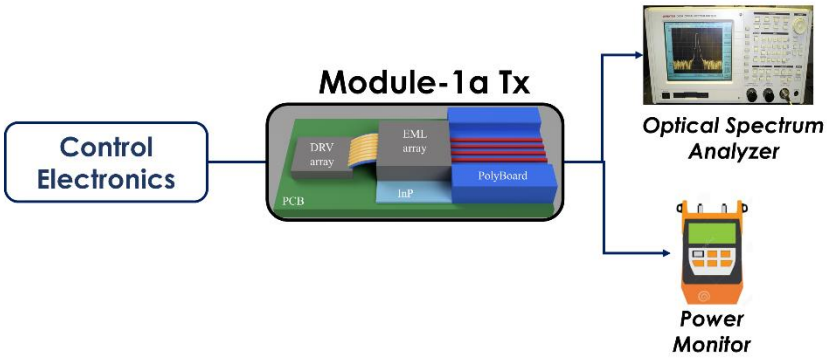

Figure 4: Indicative schematic representation of the evaluation of the optical properties of Module-1a Tx

Evaluation of the EML arrays

Each EML element of the 4-fold EML arrays within SPRINTER's Module-1a Tx consists of a distributed feedback (DFB) laser, an electro-absorption modulator (EAM) and a semiconductor optical amplifier (SOA). Therefore, the testing will initiate by carefully tuning the current values we insert at the DFB and SOA sections, as well as the voltage values we insert at the biasing section of the EAM, aiming to firstly verify the correct operations of each EML, and then to perform a mapping procedure for these 3 values, in terms of the targeted KPIs within this phase e.g., the output optical power, the side-mode suppression ratio (SMSR), the EML's output wavelength etc. Since Module 1 (both versions) operate in a parallel single-mode configuration, wavelength stability and tunability is not under the scope of interest within these tests. Furthermore, the DFB's and SOA's L-I-V curves can be obtained by adjusting the current that is being provided to the laser by the current source, read the junction voltage, and measure the output optical power with an optical power meter operating in the O-band. If deemed helpful during the testing activities, the L-I-V characterizations will be implemented for each component (DFB or SOA) under different configurations of the other section (SOA or DFB respectively to examine the influence between the sections. For the EAM section, the transfer characteristic will be determined by measuring the output optical power for fixed values of the current values of the DFB and SOA sections, as a function of the input DC voltage. In this way, key DC metrics of the EAM will be extracted, such as the slope, the linear regime and the DC extinction ratio. The aforementioned measurements constitute the DC characterization of the EML component and will be performed sequentially for each EML element of the quad array. For the CW characterization of the EMLs, an external Vector Network Analyzer (VNA) will be implemented to assess the electro-optical bandwidth of the EAM section. To that end, one optimum set of settings for the current and voltage values for the DC EML sections identified within the previous characterizations will be chosen, driving the RF input of the EAM section with the sweeping CW output of the VNA, spanning in frequencies within the identified frequency range of interest. Then, the output

light of each EML element will be coupled via the fiber array to an external O-band photodetector, down-converting the optical signal to the electrical domain, and feeding its electrical output to the input of the VNA. In that way, the frequency response of the EML will be extracted, having calibrated the response of the remaining components such as the photodetectors, RF cables, connectors etc.

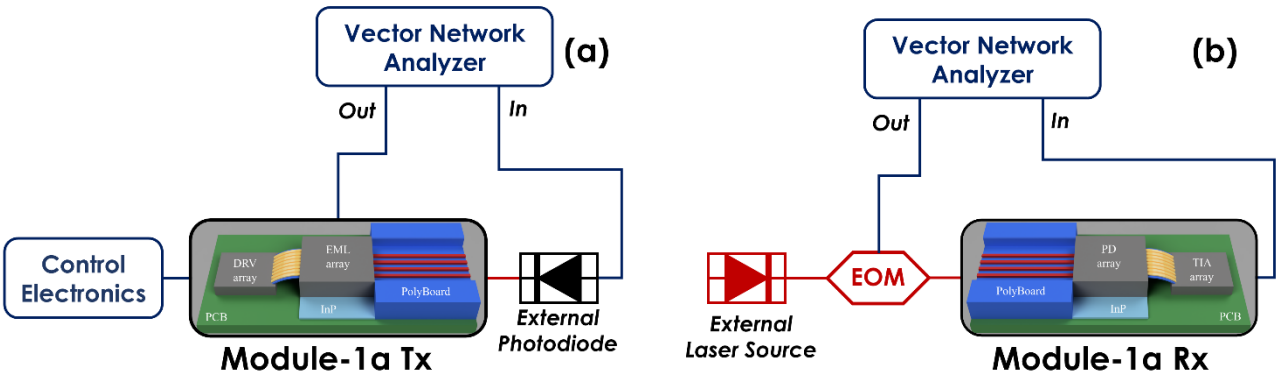

Figure 5: Indicative schematic representation of the experimental setup for the evaluation of the frequency response of (a) Module-1a Tx and (b) Module-1a Rx

Evaluation of the PD arrays

For the O-band InP PD arrays hosted in Module 1a, the characterization procedure will follow a similar rationale as for the EML arrays, but in a more simple and straightforward manner, given the reduced complexity of the prototype's receiver side. More specifically, the DC characterization of the PD mainly focuses on the extraction of the PD responsivity curve. It is important to note that the PDs fabricated at FhG-HHI are mature technology, since they are also produced as products, and therefore their expected responsivity is known beforehand. Therefore, these tests are performed mainly for validation purposes and for identification of possible issues during the packaging and shipping processes. For the extraction of the photodiode's DC responsivity curve, light from an external tunable laser source operating in the O-band will be coupled in each PD's waveguide, measuring the produced current after photodetection. Then, the responsivity will be calculated as the ratio of the measured photocurrent to the incident optical power. The CW characterization will take place similarly to the transmitter, by employing external optical components to assess solely the performance of the PD. Specifically, an external O-band laser source will act as the optical input of an electro optical modulator also operating in the O-band, driven electrically by the output of a VNA operating in a sweeping CW mode. Then, the optical signal will be fed to the receiver side of the prototype, where the on-chip PDs will generate the corresponding RF signals which will be fed to the input of the VNA. In that way, the electro-optical bandwidth of the PD will be extracted, having calibrated the response of the VNA with respect to the frequency responses of the remaining components.

System approach evaluation

For the final testing phase of the prototype, the prototype, as a whole, will be evaluated in a stepwise manner. Starting off, external photodetectors will be implemented to assess the RF performance of the transmitter side consisting of the EML array as well as the driving electronic circuits. The RF input of the EAM will be driven by NRZ on off keying (OOK) signals at 50 Gb/s, being the target within SPRINTER, using the proper software tools to extract main KPIs defined for NRZ signals such as the optical modulation amplitude (OMA), the extinction ratio (ER), the transmission and dispersion eye closure (TDEC) the relative intensity noise (RINxOMA) etc, using the appropriate experimental methodologies as defined by the corresponding standards. To enable these high-speed testing activities, an arbitrary waveform generator (AWG) and a real-time oscilloscope (RTO) will be used, capable of generating and capturing such high-speed signals, capturing the eye-diagrams in real-time, as well as providing the ability to capture the obtained waveforms to be used for further offline

processing via the appropriate software tools, extracting the estimated and the real received bit-error ratio. Then, similar processes will take place to assess the RF performance of Module-1a's receiver side consisting of the 4-fold PD and TIA arrays, extracting the same KPIs where deemed appropriate. These two steps serve as the intermediate tests for the final phase of the lab testing campaigns of Module-1a, being the evaluation of the prototype as a whole. In this phase, little to no external components will be implemented and the operation of all integrated optical units will be tested in a system oriented experimental setup. This phase in particular will contribute significantly towards the next phases of the prototype's evaluation during the system integration in the TSN-enabled infrastructure, within the Task 7.3 related activities (see 3.2) . More specifically, end-to-end measurements will be performed with NRZ signals generated by AWGs, coupled to the prototype's RF inputs, taking into consideration that the specifications of the generated signals match as much as possible those of the signals generated by the TSN NICs in order to emulate the prototype's expected performance in the final demonstration. The generated optical signals from each separate optical lane will be coupled to external fiber spools of varying length to assess the performance of the module with respect to different transmission distances within the range of interest defined by the application scenarios. These fiber spools will be connected to the receiver side of the prototype where they will be detected by the PDs, amplified by means of the TIAs and then will be coupled to an external RTO or an electrical spectrum analyser (ESA) to capture the obtained RF signals and analyse the identified KPIs discussed earlier (OMA, ER, TDEC etc) within the end-to-end evaluation. During the evaluation processes, a thorough power budget mapping the power in each point of the link will take place which will be compared to the estimated power budget performed within the Task 2.3 and Task 2.5 activities to identify possible mismatches.

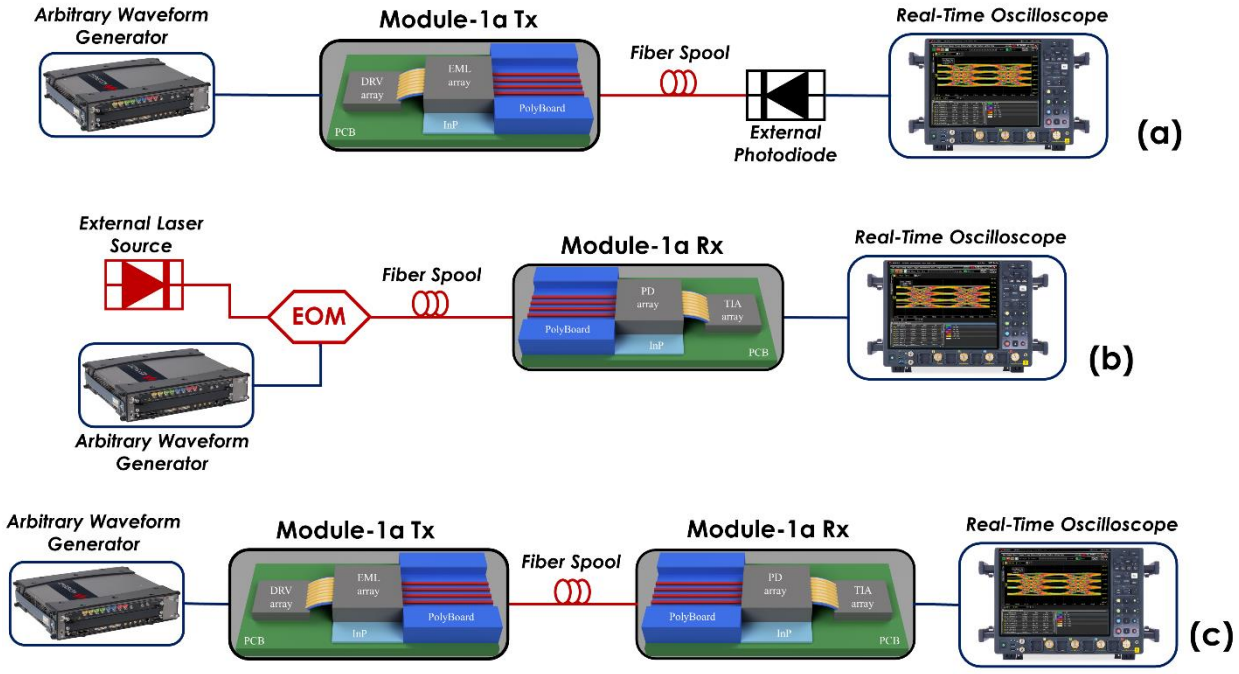

Figure 6: Indicative schematic representation of the system approach experimental setup. (a) Module-1a Tx using reference receiver, (b) Module-1a Rx using reference transmitter, and (c) Module-1a Tx & Module-1a Rx

2.1.2 Module 1b lab test

The testing of Module 1b will follow to a significant extent the same procedure as the one followed for Module 1a since the prototypes share a lot of similarities in terms of targeted transmission, and technologies. Specifically, the lab tests will initiate by the static measurements both in the optical

and electrical domain targeting, as for Module-1a, the identification of possible issues during either the packaging or the shipping processes regarding the interconnection of the PCB to the photonic chip, the hybrid coupling of the photonic platforms etc. These measurements will be performed through the same means as for Module-1a employing a multimeter with the corresponding DC circuitry for the electrical static measurements, and through the designed fiber array monitoring ports for the optical static measurements. Where necessary, specific steps tailored to the operation of the VCSELs will take place, adapting the methodology described for the EMLs. Then, for the DC evaluation, similar L-I-V curves will be obtained for the VCSELs identifying the optimum points of operation with respect to the input current, measuring the key parameters such as the output optical power, the SMSR, the VCSEL's output wavelength etc. The static transfer function of the VCSEL will take place to extract the optimum biasing point verifying operation in the linear regime. A significant difference with respect to Module-1a pertains to the temperature dependence of the VCSELs which will be studied and examined during the testing activities both in the DC and the RF characterization of the unit. More specifically, even though the prototype will employ only passive temperature cooling during the system testing activities, during the lab tests the prototype will be integrated with an external active cooling system consisting of a heatsink, an NTC thermistor enabling the temperature reading and a thermo-electrical cooler (TEC) allowing us to set the temperature with a very high accuracy. During these tests the temperature will be swept within the expected temperature range within the industrial premises where the prototype is expected to be integrated and to operate. These tests will act as a validation activity to verify the module's capability to support uncooled operation, enabling high power efficiency communications. Similar CW measurements will be performed employing external reference transmitters and receivers to measure the frequency response of the individual components. These measurements will be performed both for the transmitter and the receiver sides of the prototype, for each element of the 4-fold VCSEL and InP PD array respectively.

Then, during the testing of the prototype as a whole, the same process will take place as for Module-1a employing external AWG for the generation of the NRZ signals and an RTO for capturing the received signals. Then the signals will undergo the same evaluation process extracting the KPIs tailored to NRZ signals described previously (OMA, ER, average power, etc) under again different configurations and conditions. The configurations will differ identically to the EML case, evaluating firstly only the transmitter side, then only the receiver side, and then performing the final evaluation of the end-to-end performance of the prototype employing fiber spools in between. The conditions under which the experiments will take place will differ regarding the transmission distance (by employing fiber spools of different lengths) but also as mentioned above regarding the temperature of the VCSELs. Detailed characterization will be performed as a function of these parameters, providing significant feedback towards the final demonstration of SPRINTER technology within the Task 7.3 and Task 7.5 activities (see also 3.2). More detailed description of the evaluation methodologies is provided in subsection 2.1.1. and thus, for space economy, are not repeated here.

2.2 Module 2 test strategy

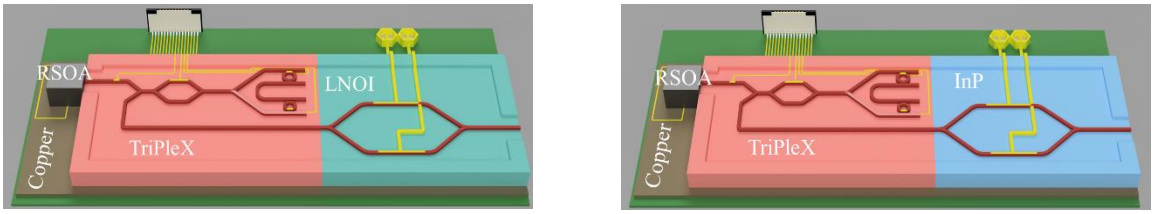

(a) (b)

Figure 7: Artistic layouts of (a) Module-2a LNOI-MZM based and (b) Module-2b InP-MZM based O-band ultra-fast tunable transmitter

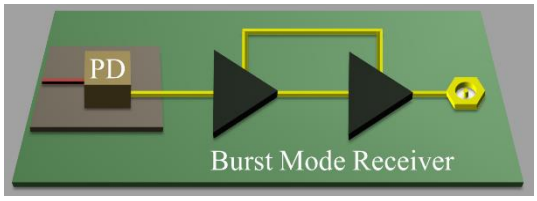

Figure 8: Artistic layouts of Module-2 burst mode receiver

Module-2 Tx consist of two main units: a) the tunable laser source and b) the MZM Modulator

Tunable laser source

The benchtop tests with focus on the ECL aim at evaluating its operation, in terms of the tunability in C-band, stability and flexibility. The first step during the characterization process of the ECLs will focus on their tunability range. More specifically, through the proper configuration of the DC voltage inputs that correspond to the heaters of the external cavity of the laser, which are responsible for the tuning of the optical source, the two extreme values (highest and lowest) in terms of the output emission wavelength will be defined, thus determining the tunability range. During that process, ICCS will perform a configuration algorithm by means of a look-up table, linking the output emission wavelength of the ECL with the corresponding DC voltage inputs, thus providing the ability to control the operating optical frequency of the optical link. Along with the tunability range, the output optical power that the ECL will be able to support will also be evaluated. To that end, an optical power monitor will be coupled externally at the output of the ECL via the fiber array monitoring port. Furthermore, the single mode suppression ratio will be computed. Finally, another key parameter under investigation is the stability of the emitted laser, both in terms of wavelength and power.

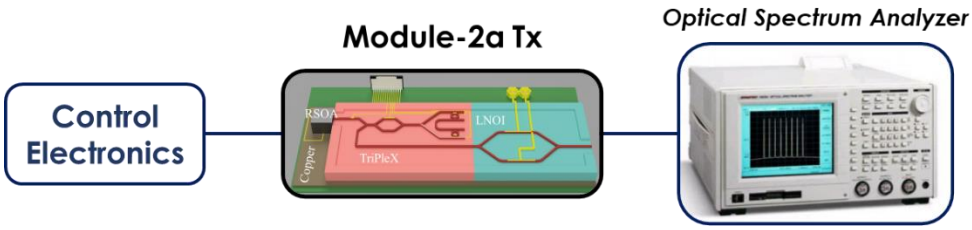

Figure 9: Experimental set-up for testing the laser source.

Modulation stage

The performance of the integrated modulators (LNOI MZM for Module-2a; InP MZM for Module-2b) will be validated. The DC characterization of the single MZM will be performed to measure the characteristic parameters: drive voltage Vπ, optical insertion losses and extinction ratio (ER). The ER is given by the optical power ratio between the on and the off state. Moreover, the frequency response of the MZM will be evaluated by employing a Vector Spectrum Analyzer (VNA) to generate the RF signal, which is applied to the modulator. The output optical signal will be detected by an external photodiode and then will be fed to the VNA RF input. In order for this measurement to provide meaningful input with regards to the operating bandwidth of the transmitter side limits, the bandwidth of the external PD should be significantly higher than the expected bandwidth of the modulator, and the frequency response of the RF components (cables, connectors etc.), used in the setup, should be calibrated.

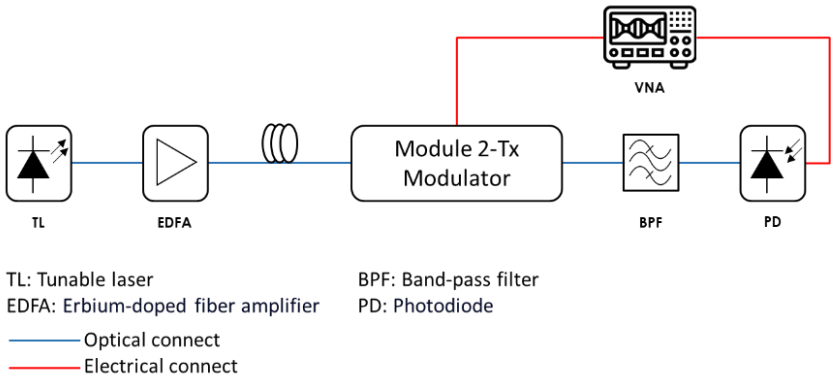

Figure 10: Experimental set-up for testing the modulation stage of Module 2-Tx

Transmission performance

In this stage the transmission performance of Module-2 Tx prototypes will be tested employing external test and measurement equipment such as external commercial PDs, Arbitrary Waveform Generators (AWG) and Real-time oscilloscopes. More specifically, an AWG will be employed to generate NRZ RF signals up to 10Gb/s which will be applied to the modulator of Module-2 Tx. The output of Module-2 Tx will be detected by an external photodiode/photo receiver that will be connected to a real time oscilloscope as in the Figure below. The data will be then offline processed, calculating important KPIs like bit error, optical modulation amplitude, relative intensity noise and transmitter eye closure.

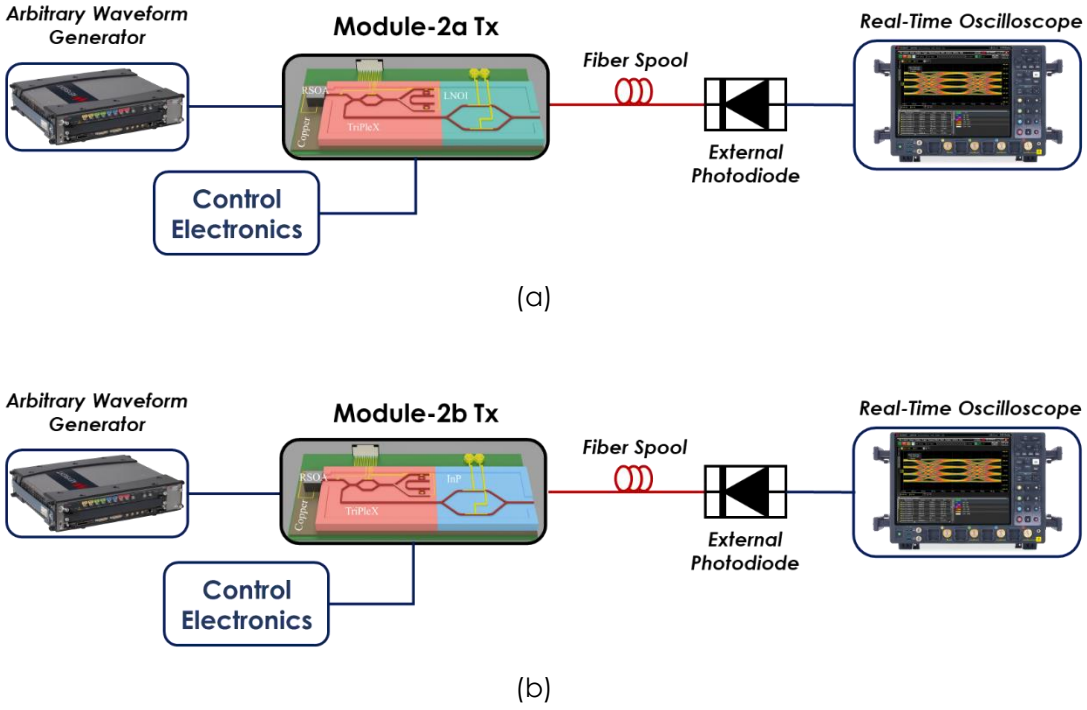

Figure 11: Experimental set-up for testing the transmission performance of a) Module 2a-Tx LNOI-MZM based and b) Module 2b-Tx InP-MZM based

Module-2 Receiver

In this stage for the benchtop characterization of Module-2 Rx prototypes, external test and measurement equipment such as an external commercial laser source (C-band), a modulator, a variable optical attenuator (VOA), an Arbitrary Waveform Generator (AWG) and a Real-time oscilloscope will be employed. More specifically, a C-band tunable laser and an MZM modulator will be used as transmitter and an AWG will be employed to generate NRZ RF signals up to 10Gb/s which will be applied to the external modulator. A digitally controllable VOA will be also connected at the output of the modulator to configure the optical power that is incident at the receiver. The output of Module-2 Rx will be connected to a real time oscilloscope as in the Figure below. The data will be then offline processed, calculating important KPIs like bit error and eye closure for different optical power levels.

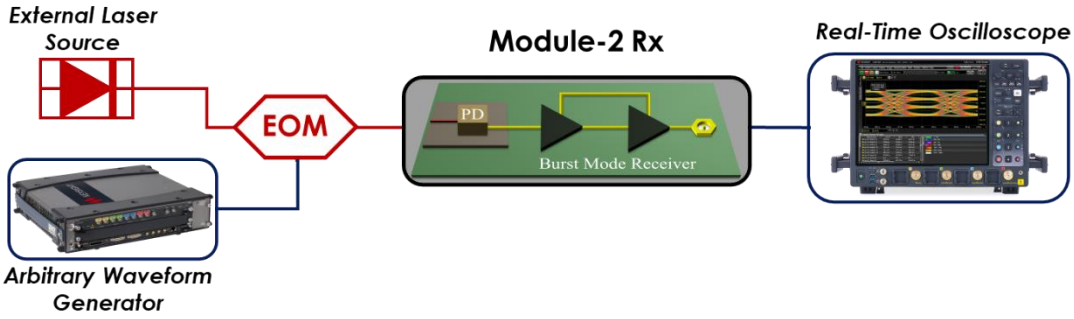

Figure 12: Experimental set-up for testing the receiving performance of Module 2-Rx

System approach evaluation

For this testing phase the end-to-end performance of Module-2 Tx and Rx will be tested. Firstly, external testing equipment will be employed. More specifically an AWG will be employed to generate NRZ RF signals up to 10Gb/s which will be applied to the modulator of Module-2 Tx and the

output of Module-2 Rx will be connected to a real time oscilloscope. Bit-error and eye closure measurements will be performed including transmission over fiber spools with length up to 2km.

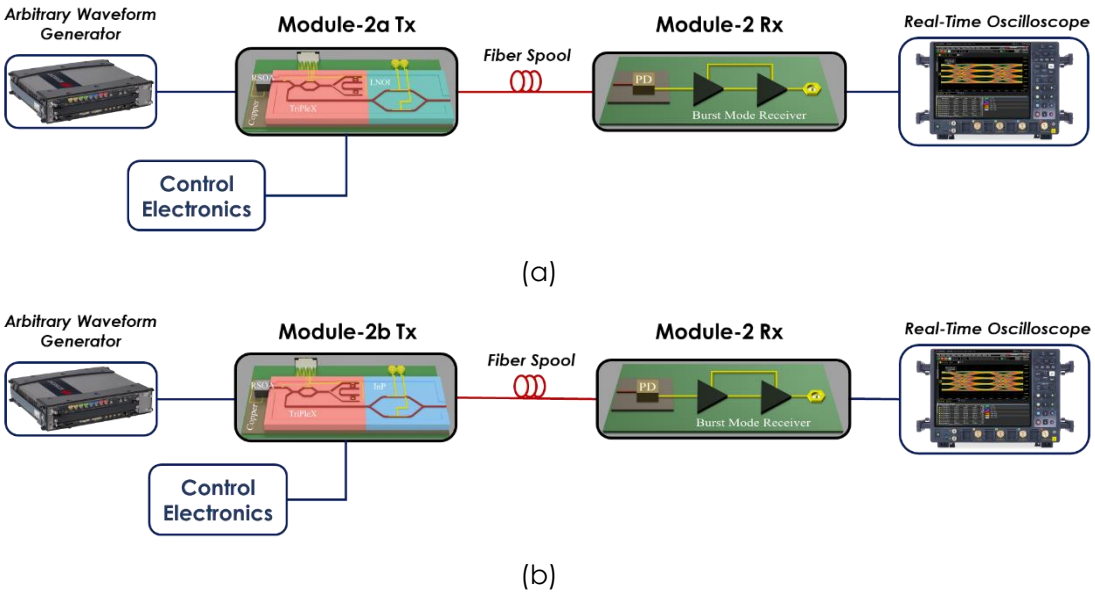

Figure 13: Experimental set-up for testing end to end performance of Module-2 Tx and Rx when the Tx is based on a a) LNOI-MZM and b) InP-MZM.

2.3 Module 3 test strategy

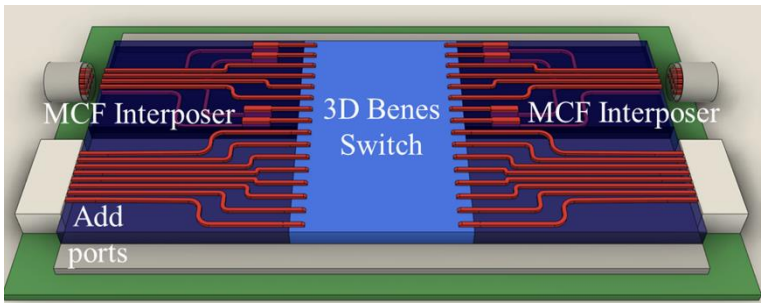

Figure 14: Artistic layout of Module-3: O-band 3D PolyBoard SDM-ROADM.

SPRINTER's Module 3 is an SDM-ROADM node consisting of a 32x32 Benes switch based on the 3D PolyBoard photonic platform, allowing for the implementation of both horizontal and vertical MMIs, allowing for high dimension switch capabilities, while minimizing the crossing sections of the optical waveguides. The switch will accommodate MCF interfaces both at its input and its output stage enabled by an MCF fan-out implemented again on the 3D PolyBoard platform, as well as interfaces of standard SMFs serving as the node's "add" and "drop" ports. This novel switching scheme will be thoroughly examined with respect to the identified KPIs pertaining to standard optically enabled switching solutions. The experimental evaluation of Module 3 will consist of multiple phases, that are described below.

Static Measurements

Similar to the testing strategy of the previous prototypes, Module-3's evaluation will initiate with static electrical measurements to verify the proper interconnection of the PCB part to the optical chip and make sure that the measured ohmic resistances of the prototype's heater-based phase actuators

are the expected ones. Then, static optical measurements will take place employing an external tunable O-band laser source, measuring the prototype's insertion loss, being the excess attenuation experienced by the optical signal during propagation in the optical switch. Insertion loss can be broken down primarily to propagation loss at the waveguides due to scattering and absorption as well as to coupling loss at the interfaces (fiber to PIC as well as polymer to silicon nitride) due to mode mismatch and reflection at the facets. Fiber to fiber loss will be measured for the SPRINTER optical switches, which is specified as $IL = 10\log_{10}\frac{P_{in}}{P_{out}}$ (in dB). Loss uniformity will be also calculated by measuring the insertion loss for all different input-output permutations of the switch. If deemed necessary during the testing activities, insertion loss will be measured as a function of wavelength to estimate the optical bandwidth of the switch. The 1-dB and 3-dB bandwidth are defined as the bandwidth where transmission remains within 1-dB or 3-dB respectively compared to the peak transmission wavelength. Under that context, a KPI under evaluation will be the polarization dependent loss (PDL), i.e., the peak-to-peak difference in the insertion loss of an optical component or system with respect to all possible states of polarization. It is expressed as the difference between the maximum and minimum insertion loss in decibels when the polarization of the input signal is varied $PDL = IL_{max} - IL_{min}$.

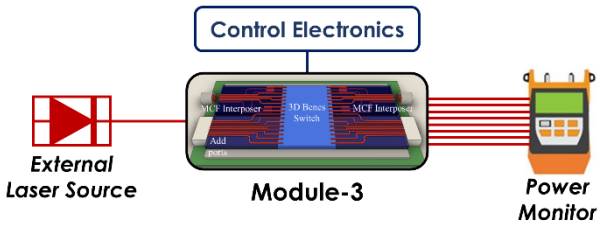

Figure 15: Indicative schematic representation of the experimental setup for the evaluation of Module-3's optical properties

Evaluation of Switching KPIs

After the aforementioned activities have been performed, the next phase will consist of standard CW-based evaluation of the prototype's switching capabilities. To that end, using the same external O-band laser source, all cross and bar states of the prototype's crossbars will be identified by measuring the power at the output ports of the module, and a detailed mapping of all actuators' states will be performed. Then, KPIs like the switch's extinction ratio (ER) and crosstalk will be extracted. ER is the ratio of peak transmission power to the minimum transmission power in an optical switch. It is reported in dB and is given by $ER = 10log_{10}\left(\frac{P_{max}}{P_{min}}\right)$. The total switch's ER is heavily reliant on that of a single crossbar, which will be measured during the fabrication testing activities held in HHI. The total ER will be measured by configuring the crossbar between the "bar" and "cross" states, measuring the optical power obtained in each case in multiple configurations. Since the ER is not infinite, optical crosstalk occurs between different switching ports which can be estimated through simulations if the average ER per switching element has been identified. At each output port of the switch, the total optical power is the summation of the designated signal routed to the specific port, plus undesired signals stemming from the crossbar's finite ER that were originally routed to different ones. Then, the switch's configuration time will be measured using the same CW laser at the optical switch input while a very fast PD will be connected at the optical outputs and at an oscilloscope. A trigger pulse will be sent from the electronic controller to the oscilloscope when the optical path is configured. The oscilloscope will measure the 10-90% rise time of the signal and the time it takes for the signal to show at the oscilloscope by the time the trigger pulse is issued. The configuration time per path of the switch will be also measured and will be compared against the switching time measured for the test building block structures.

System approach evaluation

During the final phase of the lab testing of Module-3, a system approach will be followed in the experiments, evaluating the performance of the switch with optically modulated signals. To that end, external optical equipment will be used, including an external O-band laser source, an electro-optical intensity modulator, an AWG generating the RF signals responsible for driving the modulator, as well as O-band photodetectors at the receiver side, coupled to an RTO to monitor the resulting RF signal after photodetection in real-time. According to the SPRINTER aspired architecture, Module-3 will act as an intermediary node for the interconnection of data generating and receiving nodes consisting of TSN NICs using Module-1a (O-band, EML-based) as its physical layer interface. Therefore, the testing activities of Module-3 will be performed under this context, providing and receiving feedback from the Module-1a characterization and testing activities. At the input of the switch, 50 Gb/s NRZ OOK signals optically modulated through the external O-band intensity modulator will be inserted. Then, leveraging the mapping of the switch's crossbar states the signals will be routed to the desired output, coupled to the photodetector. The electrical output of the photodetector will then be fed into the RTO, where an evaluation of the obtained NRZ signals will be performed under the scope of the KPIs described previously, in the Module 1 lab test subsection. If available during the testing activities of Module-3, the external reference O-band transmitter and receiver will be replaced by the Module-1a transmitter and receiver prototypes, using fiber spools of the appropriate length to emulate the final demonstration scenario of SPRINTER technology. As a final step, the manual routing of the optical signals will be replaced with the configuration algorithm of the Benes switch developed within Task 2.5 by ICCS, implementing this algorithm in an FPGA platform controlling the voltages inserted in each crossbar, allowing for the automation of the routing schemes. Detailed reports on these algorithms will be reported in Deliverable 2.4 due for the project's M22.

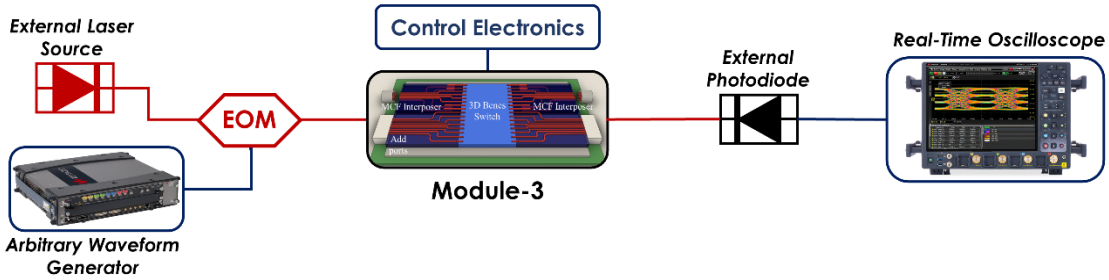

Figure 16: Indicative schematic representation of the system approach experimental setup for Module-3 using external optical transmitter and receiver.

2.4 Module 4 test strategy

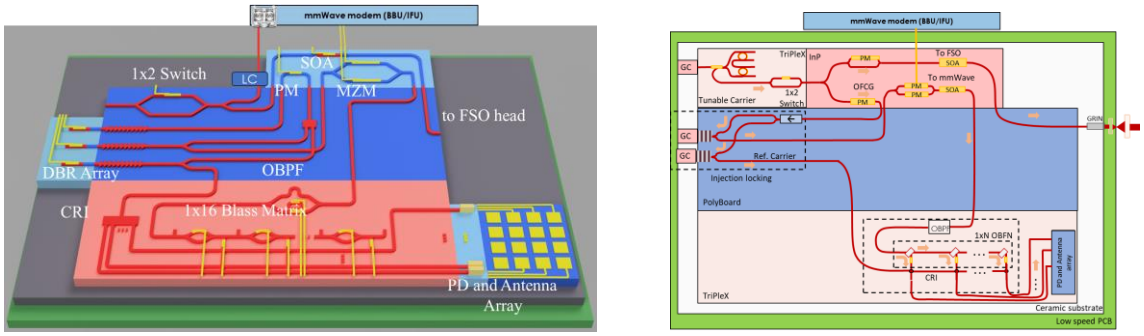

(b) (b)

Figure 17: Artistic layout of a) Tx part of the hybrid FSO/mmWave of the fixed node transceiver and b) Tx part of the hybrid FSO/mmWave of the remote node transceiver

2.4.1 Module-4 Tx

The transmitter of both remote and fixed node (Module-4 Tx) will be based on the hybrid PolyBoard/InP/TriPleX platform. The benchtop characterization of this module is focused on the thorough characterization and testing of the following main optical units/stages of the module. Detailed information regarding the operation of Module-4 fixed node and remote node transceivers are reported in SPRINTER Deliverable D2.1.

Tunable Laser Sources

Module-4 Tx (fixed node (FN) and remote node (RN)) modules will comprise 3 tunable lasers (TL). For the mmWave operation (FN & RN), the first TL will serve as the input to the optical frequency comb generator (OFCG), whereas the rest ones will be part of the injection locking process to stabilize the output RF frequency and minimize the phase noise of the emitted signal. For the Module-4 Tx RN node when operating with the FSO system, the optical carrier of the first TL will be routed to the FSO modulation unit (InP MZM and SOA) instead of the OFCG, employing an integrated 1×2 MZI crossbar switch. For the benchtop testing of the optical sources the same procedure as in Module-2 will be followed.

Optical Frequency Comb Generation stage

The optical frequency comb generator (OFCG) serves as the first part in the phase locking mechanism unit. It consists of two phases modulators with high analog bandwidth, integrated on an InP chip. The output of the first ECL laser will serve as the input to the OFCG circuit, long with two sinusoidal electrical signals, each one feeding the respective PM. The field at the output of the OFCG resembles a comb, consisting of multiple generated frequency tones, and will serve as an input to the rest of the ECLs to lock their phases, during the injection locking process. During the benchtop tests for the characterization of the OFCG, the circuit will be isolated via the monitoring ports, to better assess its performance and extract the correspondent KPIs. Specifically, for the OFCG, the key parameters that will be evaluated will include the performance of the PMs (DC characterization, frequency response), the range of the frequency comb, defined as the range over which all the frequency tones remain over a specific power threshold. Furthermore, the tunability of the OFCG will

be also evaluated since it defines the flexibility of the possible generated frequencies. Finally, the resolution of the OFCG will be considered, defined as the minimum frequency step between two successive frequencies tones able to be generated. Finally, the optical frequency comb's ability to generate frequency tones that can be used to phase lock two lasers with frequency difference of 71GHz to 86GHz (E-band) will be evaluated. The field at the output of the OFCG will be directly monitored via an output port from the fiber array, fed into an optical spectrum analyzer (OSA).

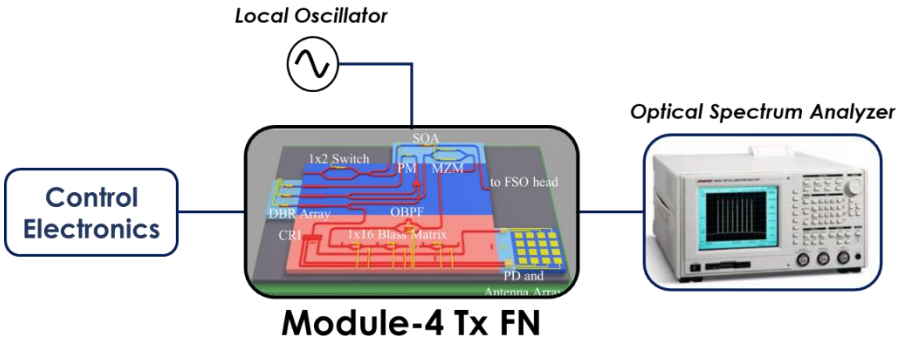

(a)

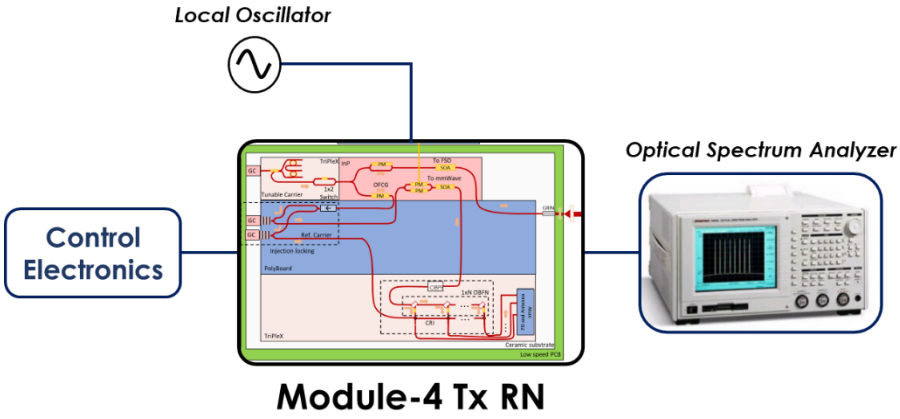

(b)

Figure 18: Experimental set-up for testing the optical frequency comb generator of a) Module-4 Tx FN and b) Module-4 Tx RN

Injection Locking stage

The output of the OFCG will be injected in the ECLs during the injection locking process, serving as the second and final part of the phase locking mechanism. As a result of this mechanism, the phases of the optical signals are locked leading to a significant decrease of the phase noise of the generated RF signal after the photodetection process. Especially in the case of mmWave signal generation, phase noise can be a strongly limiting factor highly affecting and degrading the quality of the signal at the demodulation stage. Therefore, the use of a phase locking scheme is rendered necessary, serving as an efficient solution to this issue.

Regarding the characterization of the injection locking process, the verification of the phase locking will be conducted via the monitoring port before the photodiode (PD)whilst also monitoring the electrical output of the PD. More specifically, in all modules a monitoring port of the optical signal before the PD will be implemented which will be externally coupled to a low resolution OSA for the alignment process between the OFCG and the DBR output frequencies. The RF output of the PD will be also separately monitored using a high bandwidth Real Time Oscilloscope (RTO). After the locking

of the lasers has been realized, the limits of the phase locking process regarding the frequency detuning will be examined. Furthermore, a quantization of the linewidth reduction of the beating term tone after the photodiode will be also realized. The frequency stability of the produced RF tone will also be examined within this context. Finally, extensive experiments will be performed comparing the operation at the free-running mode of the lasers versus the injection locked operation, in order to determine the effect of the phase locking mechanism, using high-order modulation schemes.

Modulation unit

Module-4 Tx fixed node will be equipped with an InP MZM followed by an SOA for the mmWave operation and the Module-4 Tx remote node with two InP MZM modulators followed by an SOA for each MZM, one for the mmWave operation and one for the FSO operation. The same characterization process as in Module-2 Modulation stage will be followed, employing the monitoring ports that have been included in the designs of this module.

Filtering unit

The optimum values regarding the applied voltage for the bias of the electrodes of the SSB-SC filter are defined, targeting high extinction ratio as well as spectral flatness of the passbands. The extinction ratio of the filter will be determined, defined as the difference in decibels between the power of the passband and the stop-band state of the filter. The proper configuration of the optical filter is focused on maintaining the highest possible extinction ratio, while having flat passband and stop band responses. The characterization of the filtering unit is performed both in a static configuration employing wideband optical input signals to extract the transfer function, and in a dynamic configuration employing modulated signals and verifying the suppression of the unwanted spectral content. For the optical filtering unit's configuration, the fiber array port corresponding to the input and the filter's output will be used. In the following figure a schematic of the set up for the testing of the filtering unit employing VNA is presented.

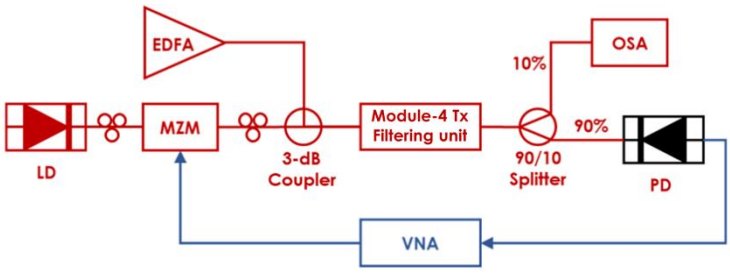

Figure 19: Experimental set-up for testing the filtering unit of Module-4 Tx.

Optical Beamforming Network (OBFN)

The beamforming unit will be based on the Blass matrix architecture and will accommodate the formation of 1 beam with 16 (4x4) antenna elements. The matrix will comprise a set of longitudinal and lateral waveguiding lines inside a crossbar topology and will use a set of MZIs as tunable couplers for the cross-connection of these lines. In this stage the basic functionality of the OBFN will be evaluated with respect to the ability to impose the required phase shift in each optical path and achieve the desired steering. Under this context, a detailed characterization of the crossbar and 3-dB states of the MZIs, comprising the Blass-matrix OBFN, is performed. In order to determine the range of feasible steering angles, as well as its ability to successfully steer the information signal at the desired target angle, which is the ultimate goal of this unit, offline experiments will be performed, implementing the beamforming configuration algorithms that will be developed.

Photonic up conversion and emission unit-mmWave

This unit's benchtop testing is focused on the static characterization of the PDs that act as photonic upconverters and the semiconductor optical amplifiers (SOAs) included before the PDs. This unit's performance will be evaluated in the transmission testing phase using Module-4 Rx too.

FSO emission

For the FSO operation the optical signal is connected though the fiber array to a to a fiber-pigtailed telescopic lens system, based on commercially available off-the-shelf (COTS) components that facilitate its transmission. The performance of the telescopic lens system will be firstly tested with external test and measurement equipment such as external commercial PDs, lasers, modulators, Arbitrary Waveform Generators (AWG) and Real-time oscilloscopes in different propagation distances.

2.4.2 Module-4 *Rx*

The receive path of Module-4 will consist of a horn antenna, an RF Unit which will include all the E-band circuitry along with the ADC, and the Baseband Unit. The antenna will be mounted through a WR12-type waveguide interface, on the housing of the BB/IF/RF Unit. The receive path of Module-4 will operate in the 71-76/81-86 GHz ranges. Except for the horn antenna, the receive path will be based on a commercial grade, E-band platform from ICOM. Validation of the Module-4 will be performed first in standalone tests, and then in integrated tests.

In parallel, the BB/IF/RF Unit will be tested in loopback and point-to-point link modes. To this end, an E-band transmitter equipped with a horn antenna, developed by ICOM for SPRINTER validation, will be used. These tests will be performed in two stages: first, the link will be validated at the physical layer, measuring the main performance parameters such as the received SNR, the achieved highest modulation type and the L1 throughput, via ICOM's E-band monitor SW platform. After the successful completion of this phase, testing at the second stage will focus on measuring performance with data traffic, at L2-L4 (e.g. iperf). The setup is shown in Figure 20.

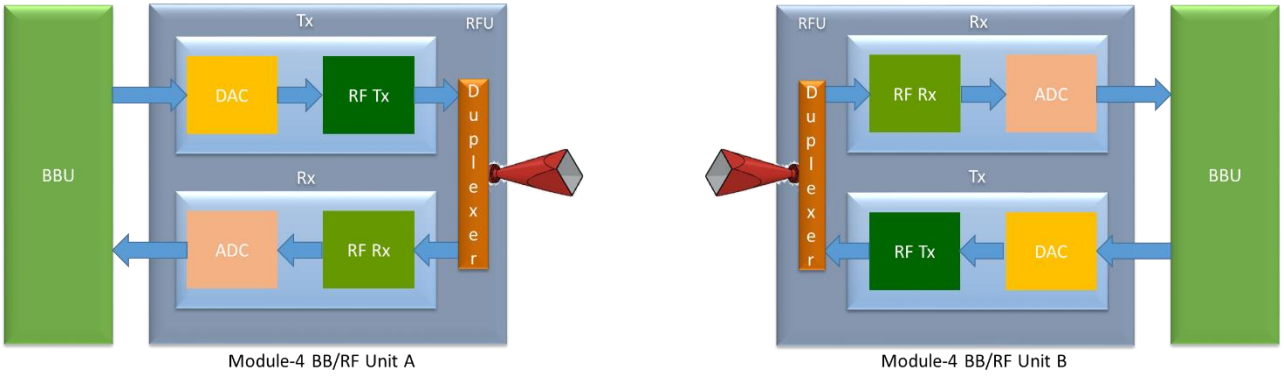

Figure 20: Module-4 BB/IF/RF Unit Test Setup

The photonic part of the Module-4 FN receiver is depicted in Figure 21. For the mmWave operation case, at the PIC level, a fast ECL source will be deployed to generate an optical carrier with the desired emission wavelength while an InP MZM will be used in the optical modulation stage. The MZM will be driven by the demodulated 10 Gb/s OOK-NRZ signal that will be provided by the baseband unit. When operating with the FSO system, the received signal will be coupled to the hybrid PIC, using a fiber pigtailed telescopic lens system, like the transmitting side. The same testing methodology as in Module-2 Tx will be followed.

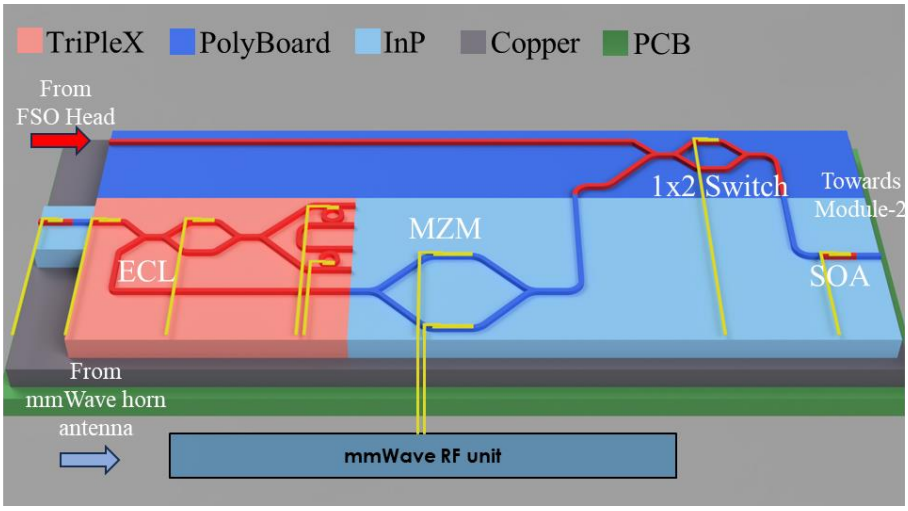

Figure 21: Module-4 Rx FN

2.4.3 Module-4: Transmission performance evaluation

This phase builds on the initial testing phase of Module-4 Tx and Rx hybrid FSO/mmWave transceivers by conducting wireless transmission tests to assess and characterize their transmission performance. In this phase Module-4 will be integrated with the Baseband/IF unit (Module-4 Tx - mmWave link) developed by ICOM for the mmWave link and the network interface cards (NICs) provided by NVIDIA for the FSO link.

Firstly, the transmitter and receiver modules will be placed in parallel and on the same height with the aid of properly configured mounts of adjustable elevation and azimuth angles validating the possibility of Module-4 to establish a wireless FSO/mmWave link. After the proper alignment of the Tx and Rx modules, and the establishment of the wireless link the transmission performance of Module-4 will be tested in terms of received power, bit error rate, error vector magnitude. These measurements will be performed for mmWave and FSO carriers for diverse distances. In addition, the performance of the real time digital signal processing algorithms that will be employed in order to guarantee the quality of the link will be tested. Finally, within this phase the steerability of the OBFN will be evaluated. At this stage the initialization and the alignment of the link will be performed employing the beamforming unit. The receiver will be placed in different positions testing the ability of the optical beamforming network to successfully steer the information signal at the desired target angle while also testing the performance of the developed beamforming configuration algorithms. In Figure 22 the testing set up for the mmWave case is depicted.

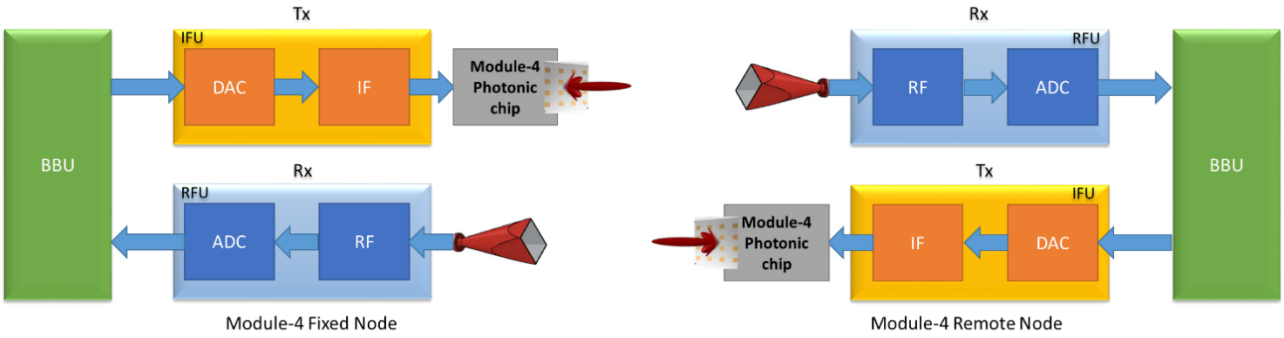

Figure 22: Integrated Module-4 Test Setup

3 SYSTEM INTEGRATION AND VALIDATION

This chapter is intended to provide a detailed description of the integration phase that follows the module level test activity.

This system level test activity is divided in three phases, namely: (i) Network component test (described in 3.1) where NVIDIA TSN NICs are integrated with CMC controller in CMC lab; (ii) 5G TEI validation lab test, where SPRINTER TSN backbone is verified in a RAN fronthaul connection (described in 3.2); (iii) ICCS validation lab test, where different local machine cell types are evaluated (described in 3.3).

The scope of this system level test activity is to guarantee interoperability of HW and SW modules and architectures developed inside the project and their adherence to target KPI before the industrial application test phase is run.

3.1 Network components test

The objective of the Network Component Test is to substantiate the working of the NICs and the TSN control plane. In addition to the working of the control plane data, the traffic is tested with priorities. The requirements of slot duration, packet transmission time, data transfer rate is considered as well. In addition to the existing performance of the system, the tests would be performed in future to scale to achieve more bandwidth.

NIC (Network Interface Cards) are provided by Mellanox for their datasheet see [6].

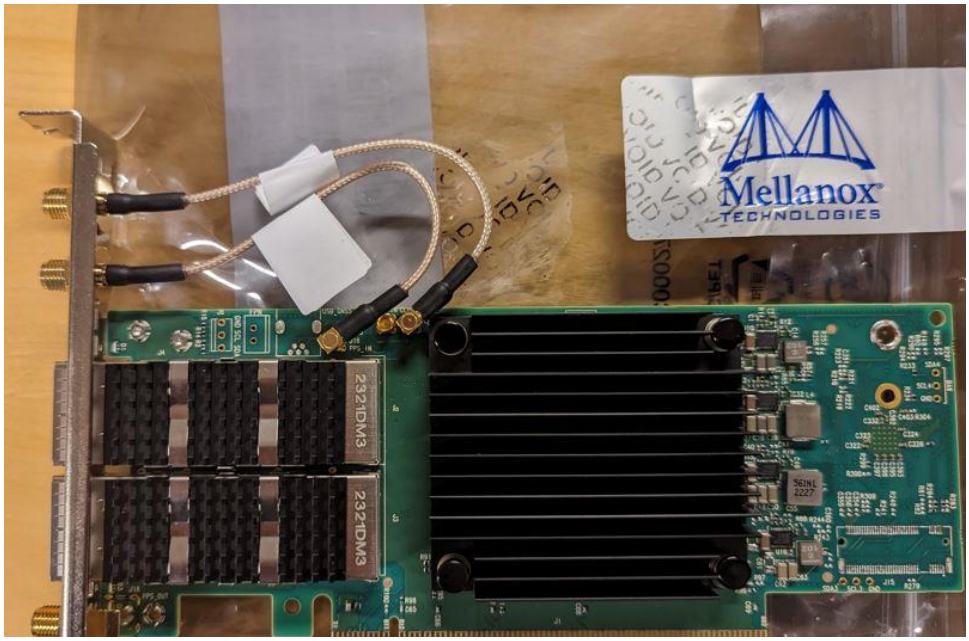

Figure 23: SPRINTER NICs by MLNX

These NIC cards have PCI-e slot dual port 100Gb/s data support that require passive cooling. These come with a sophisticated heat dissipation fan and expects the hardware that is running on to generate enough airflow to cool it down. High level environmental and thermal requirements for a server hosting TSN NICs in ConnectX-6 card format can be found in [7]; the same host shall have high-end CPUs with at least 64 cores/128 threads.

Cumucore chose and ordered a custom Supermicro which has characteristics in line with requirements.

Figure 24: Custom hardware at Cumucore laboratory to support NICs by MLNX

The driver stack for NICs was Linux based and hence Ubuntu Server 20.04 was installed. Similar Server was installed as a replica to the original one. One of the servers made the transmitter and the other receiver. Both servers were interconnected with QSFP DAC (Copper) Cables.

MLNX OFED(InfiniBand) software was installed to tweak the embedded performance and work with the NICs. Software to test the Control plane was provided by MLNX. The receiver and the transmitter software were installed in respective servers. The host server would run a Grand Master Clock using the OS system Clock. The custom NICs provided by MLNX would have their own internal clock. We run the phy2sycs software that will run with the Grand Master Clock. A reference would be taken for synchronisation. The goal is for each server in the system to align their internal clocks over Ethernet and then each MLNX NIC aligns each internal clock with the local server host clock. MLNX NICs can be used to relay synchronization traffic if one of the two available ports is free in the setup. For the current testing in this deliverable, we are using one port per NIC for synchronizing the clocks and the other acts as testing for the slotted traffic.

Next, we run a python script to start the dpdk (data plane development kit) script to the ethernet interface that provides timing aware ethernet internal interface. This initializes and configures the required environment before running applications that leverage for high-performance packet processing. Once this is done, the control plane testing is possible. To add to the data plane testing priority to the packets were added. Additional script was run that brought up the necessary environment, so the host and recipient were ready. On the receiving side, debugger interface was present which showed the received DSCP field of the arriving packets. Figure 25 below shows the final p2p testing setup and integration with CMC controller. One of the sides is designated as in debug mode and observes the received packets to recover and report the timing slotted schedule it observes.

Finally, a script for generating data was started on the generator side. A mix of DSCP traffic was arranged in slots and transmitted accordingly, so the receiver ends up having them in required order.

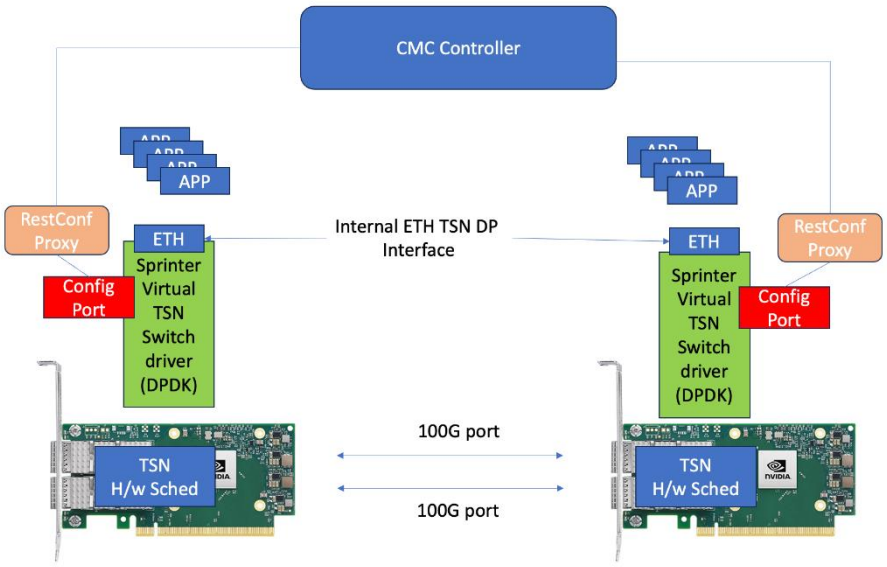

Figure 25: Control plane data flow between the transmitter and the receiver MLNX TSN NICs

The KPIs targeted for the project are: (i) minimum slot duration which we want to keep below 100us. (ii)Each packet is transmitted with 40ns accuracy within a timeslot. (iii) Line rate at 300 M bits/sec/CPU thread. This should linearly scale as we add more CPUs until the system memory bandwidth is consumed.

These tests with the NICs hosted on the server are initially done in MLNX lab. However, the tests will be repeated in Cumucore as part of deployment experience. Next, they would be verified against the Centralised Network Controller (CNC) developed by Cumucore to ensure the traffic control and apply the required network policies. Traffic control could include the discovery, prioritization, distinguishing flows by various pre-defined parameters (such as delay, error rate, resources assigned). CNC will interact with the NICs through the SDN agent (via REST APIs) that is installed on the host machine. This later would be extended to support new radio technologies and FSO type of connections.

3.2 TEI 5G end to end validation lab test

Purpose of the end-to-end test in TEI is to validate the TSN backbone connectivity that includes modules 1 a, 1b and 3 as defined in SPRINTER Architecture in an application with tight requirements of latency like the 5G Radio Access Network Fronthaul. At the same time, the tests performed in this technological context could further extend the field of application of the developed modules (i.e. Radio Access Network).

The testbed used for this validation is an E2E mobile Network based on Ericsson technologies implementing real services in a private environment. The solution is based on an 5G NSA (non-stand-alone) architecture where LTE is providing the control plane and data plane traffic while the 5G NR (New Radio) is providing the data plane to increase available bandwidth.

A representation of the laboratory components located in TEI Genoa premises is showed in Figure 26.

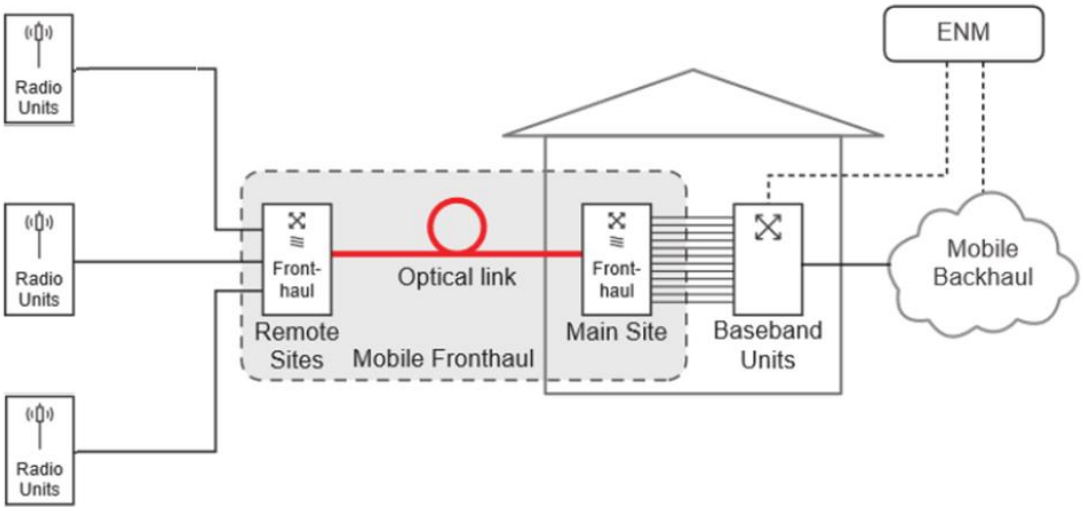

Figure 26: RAN Network in TEI E2E Lab

With reference to Figure 26, the RAN nodes identified to validate the SPRINTER components, are the baseband 6648 (Baseband Unit) and the Radio AIR6419 (Radio Unit) while the Fronthaul nodes (Remote and Main Sites) are two NVIDIA 2x100G TSN NICs hosted on COTS server; the two NICs face optical link with SPRINTER modules under test (module 1-a, 1b and 3).

Baseband 6648 (see Figure 27) provides RAN computation and has been optimized to fit all site types and traffic scenarios, supporting 4G, 5G, New Radio and IoT (mixed mode). It has a maximum backhaul throughput of 10-15Gbps in downlink and 3Gbps in uplink and up to 12 Radio Interface port operating at up to 25Gb/s (CPRI or eCPRI format) [5].

Figure 27: Ericsson Baseband 6648

AIR 6419 (see Figure 28) is an Antenna Integrated Radio (AIR) unit for 5G mid-band TDD. It has 64 transmitters and 64 receivers, 192 antenna elements, 200MHz total carrier bandwidth and an Advanced Antenna System (AAS) for Massive MIMO.

Figure 28: Radio AIR6419

It is connected to the baseband through up to 3 optical lanes working at 25Gb/s eCPRI frame format.

Both Baseband 6648 and AIR6419 are part of Ericsson 5G RAN portfolio (more info it can be found in [9]).

The network segment where module 1a, 1b, 3 and NVIDIA 2x100G TSN NICs, as part of SPRINTER TSN backbone network, will be located is the so called Fronthaul network, i.e. the one that connects Baseband Processing Function located on Baseband units (BB6648 in our case) and Radio Function located in Antenna Integrated Radio unit (AIR6419 in our setup). The tests will be focused to assess various network KPIs including latency, throughput, jitter, network reliability in two different Use Cases (UC) described in the following. The tests will be executed using *iperf* tool to measure the network performance metrics, and *ping* to test the reachability of remote node, and measure the round-trip time between BB and Radio nodes. A more detailed KPI description is provided in Table 1.

Table 1: Module-1a/b end to end testing: KPIs

KPI ID	KPI1
KPI	End-to-End Latency.
Description	Measured round-trip-time (RTT) from the moment the IP ICMP Echo Request packet leaves the User Equipment connected to the mobile Network until the IP ICMP Echo Reply is received from the destination host placed at the edge of the Network.
Data Needed	Time from Source to Target Device (i.e. measured at the communication interface). Result will be compared with same measure without SPRINTER TSN backbone network on Fronthaul connection
Owner	TEI

KPI ID	KPI2
KPI	Reliability
Description	The percentage (%) of the amount of sent packets successfully delivered to a given system node divided by the total number of sent network layer packets.
Data Needed	Packets Successfully Delivered, Total Number of Packets.
Owner	TEI

KPI ID	KPI4
KPI	Bandwidth
Description	Throughput (Downlink and Uplink) measured by a single User connected to the mobile Network connecting to a server in the Edge of the CORE network.
Data Needed	Throughput measured with and without SPRINTER TSN Backbone in fronthaul connection
Owner	TEI

KPI ID	KPI5
KPI	Packet delay variation
Description	The variation in the delay of received packets between User Equipment connected to the mobile Network and the host placed at the edge of the Network
Data Needed	Timestamps at packets transmission, timestamps at packets reception
Owner	TEI

Tests will be executed on a single user equipment (UE) connected to 5G RAN network through its air interface while transmitted/received data are crossing SPRINTER TSN backbone network on RAN fronthaul 25Gb/s eCPRI frames from BB6648 ports to AIR6419 ones.

For the test execution two different link topologies and consequent setups for SPRINTER TSN backbone were identified.

In both cases it is required to have two COTS servers (one on radio side and another on BB side) equipped each one with two TSN NICs one equipped with commercial SFP28 to ensure connectivity towards Radio/BB and the other hosting module 1a/b. Traffic connection between the two NICs is provided by PCI express (PCIe) bus on the COTS server as described in Figure 29: NIC to NIC connectivity

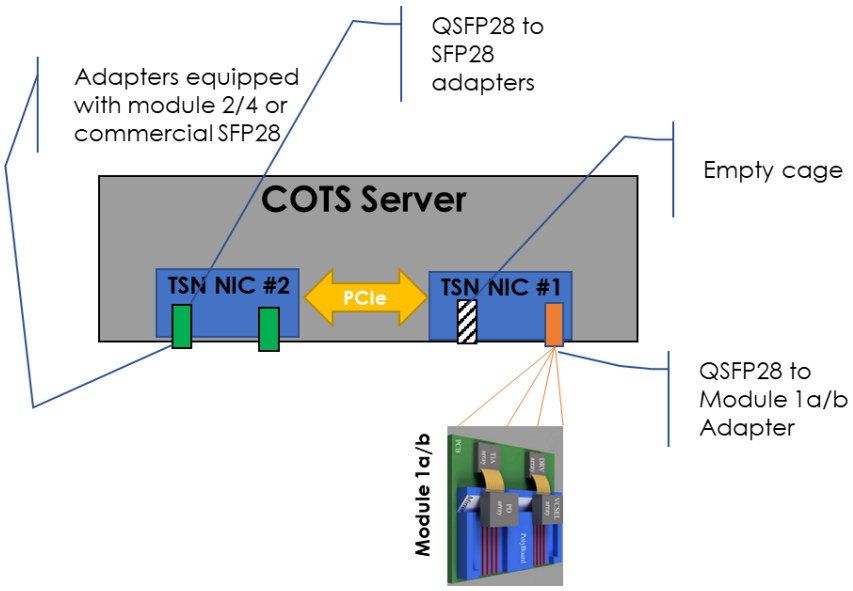

Figure 29: NIC to NIC connectivity

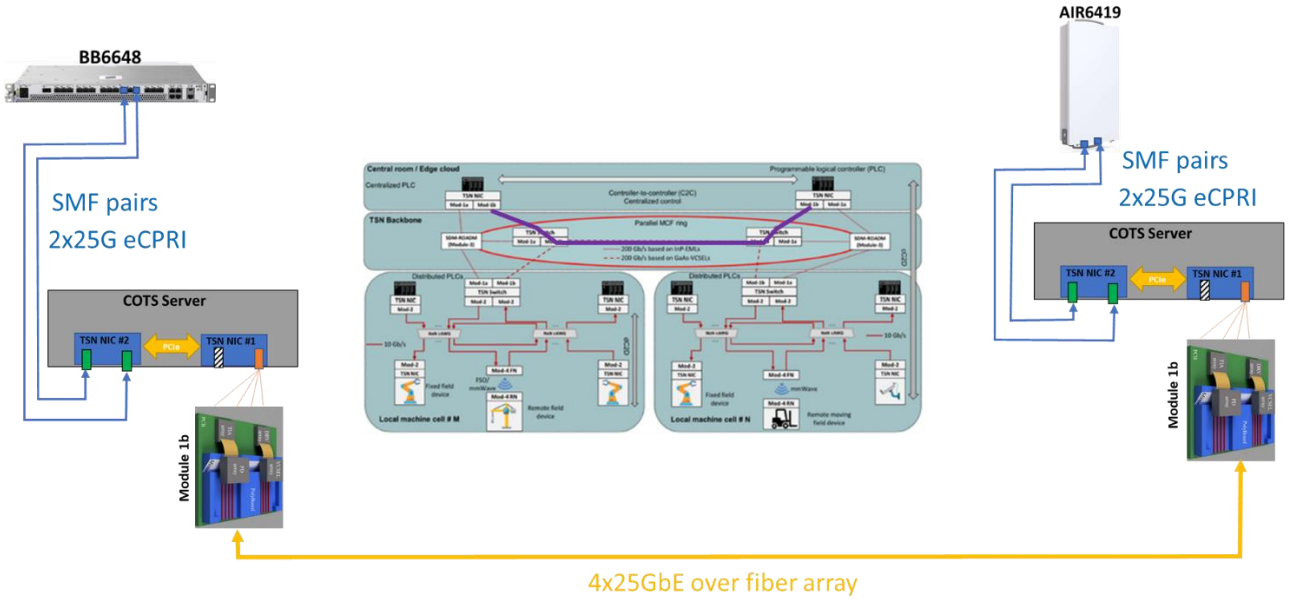

Figure 30: BB6648 to AIR6419 connectivity via TSN network, topology 1: direct connection

In the first topology, described in Figure 30, FH network is realized with two NVIDIA 2x100G TSN NICs hosted on two COTS servers, one collocated with BB6648 and the other with AIR6419 respectively, AIR/BB 25Gb/s eCPRI ports (two per Radio Unit) can be connected with TSN NICs using commercial 25G SFP28 hosted on NIC#2 ports as reported in Figure 29. Commercial SFP28 can be hosted on NIC ports by mean of an QSFP28 to SFP28 adapter (see Figure 31 and [8]) commercially available.

Figure 31: QSFP28 to SFP28 adapter

The connection between the two NICs is done wiring module 1b to the second 100G QSFP28 port of each NIC by means of an electro-mechanical adapter (developed inside SPRINTER project as part of T7.2, see Figure 32) and then through a parallel fiber array link between the two optical modules.

To be noticed that the physical layer speed of each of the four lanes of module 1b is limited by QSFP28 NIC port to 25Gb/s while TSN functionality on NIC application layer can be enabled for a maximum of 10Gb/s with the current implementation; this must be considered in Radio and Baseband configuration.

Topology 1 is meant not to test Module 1b at full speed (this is done at module level lab testing phase described in 2.1.2) but allows to verify fronthaul link establishment and stability and measure KPI reported in Table 1.

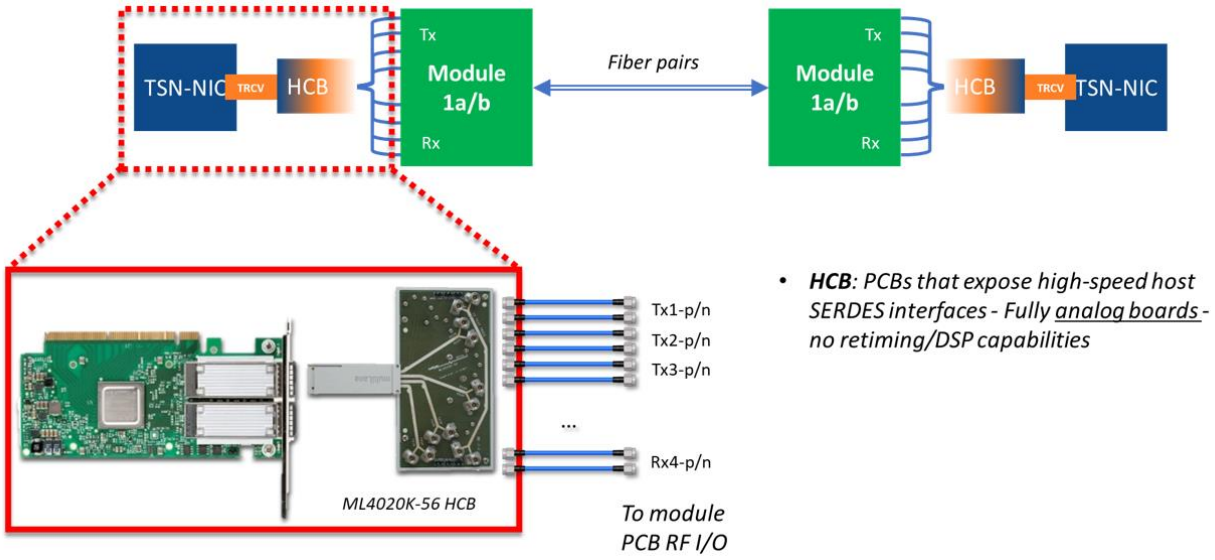

Figure 32: QSFP28 to Module 1a/1b electro-mechanical adapter

A different topology that makes use of module 1a and 3 is described in Figure 33 and it is referred in the following as topology 2 (Figure 33).

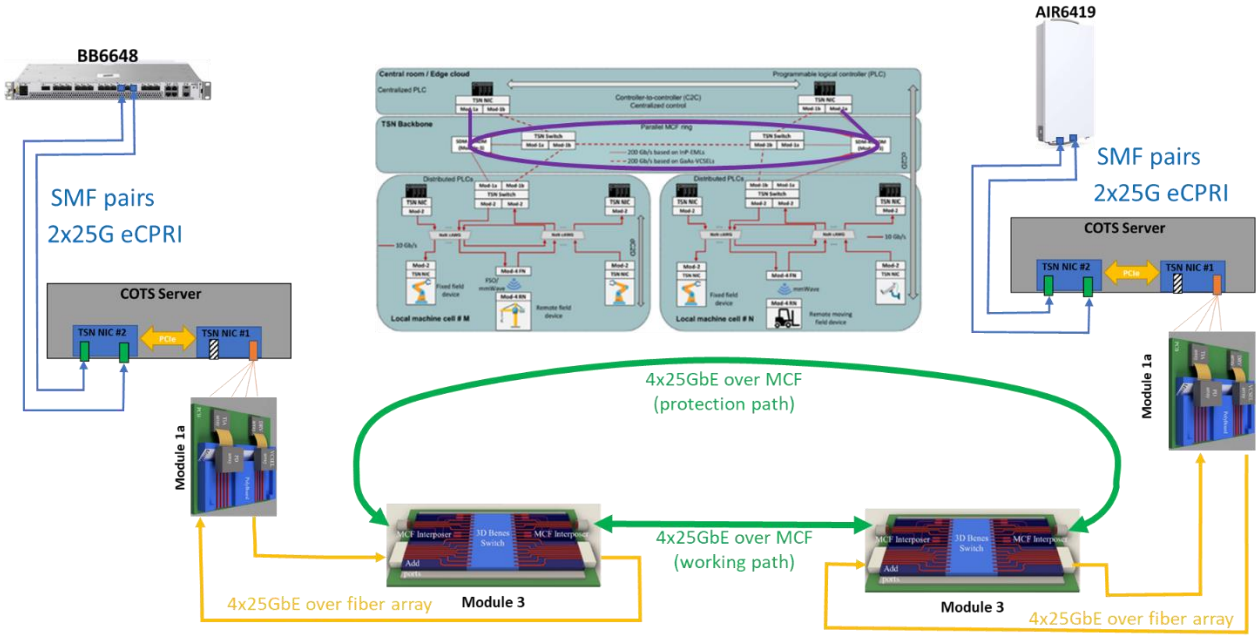

Figure 33: BB6648 to AIR6419 connectivity via TSN network, Topology 2: ring connection

In topology 2, COTS servers, TSN NICs, connections towards BB/AIR units and QSFP28 electro-mechanical adapters are the same of topology 1 setup, while module 1b is replaced by module 1a.

Module 3 is a stand-alone module with its own control electronics and control interface accessible through a dedicated GUI. The two Module 3 on the two link sides have their add/drop ports connected through fiber ribbon to modules 1a on and they are connected each other through multicore fiber (MCF) with two optical paths (working and protection).

Topology 2 presents the same figures in terms of speed of physical lanes and TSN application layer payload limits highlighted in topology 1.

Topology 2 is meant not to test Module 1a at full speed (this is done at module level lab testing phase described in 2.1.1) but allows to verify fronthaul link establishment and stability and measure KPI reported in Table 1 as per topology 1.

In addition to topology 1, topology 2 allows measurements on path protection and resilience of Fronthaul link to path variation thanks to the presence of the optical matrix inside module 3; this will assess exploitability of SPRINTER TSN backbone ring network in RAN domain.

3.3 ICCS end to end validation lab test

The experimental facilities at the ICCS 5G testbed offer a multi-access network environment for wireless experimentation. The ICCS 5G platform is composed of various 5G stack implementations including open-source and closed-source solutions for the radio access network (RAN), the 5G Core Network (CN), as well as the software stack at the users' equipment (UE). Particularly, for the RAN we exploit Open Air Interface (OAI) [2] for 4G and 5G new radio (NR) access, which is opensource, driven by fully reconfigurable and open software defined radio (SDR) equipment i.e., USRP B210 and USRP N310 devices. Currently we support up to 5 cells based on the OAI RAN hosted at the ICCS lab. Additionally, for the RAN, we utilize the licensed stack solution based on Amarisoft [3] classic box that can support up to 3 additional cells. For the 5G CN we operate with 3GPP-Compliant 5G Standalone (SA) network implementations based on the opensource solutions of OAI and open5GS [4], as well as the licensed Amarisoft CN stack. All components can be easily combined, e.g., OAI RAN with Amarisoft CN (or vice versa).

Emphasis is given on (far-)edge and cloud computing capabilities with the integration of micro-data centre infrastructure nodes at each radio access point i.e., the 4G/5G small cells, including GPU processing capabilities based on server GPUs such as NVIDIA RTX 3090 and NVIDIA A30, as well as embedded computing boards such as NVIDIA Jetson devices designed for artificial intelligence (AI) and machine learning (ML) applications, especially in far-edge computing environments where processing power needs to be balanced with energy efficiency and size constraints.

The ICCS 5G platform follows the cloud native principles for building applications that are scalable, resilient, and agile, typically built as microservices, packaged in containers, and managed dynamically, supporting day 0 to day 2 lifecycle management (LCM) operations via kubernetes and other popular orchestration engines. Figure 34 illustrates a high-level overview of the software suite enabled by ICCS 5G platform, supporting Software Defined Networking (SDN), Network Function Virtualization (NFV), Management and Orchestration (MANO) of network services and service components.

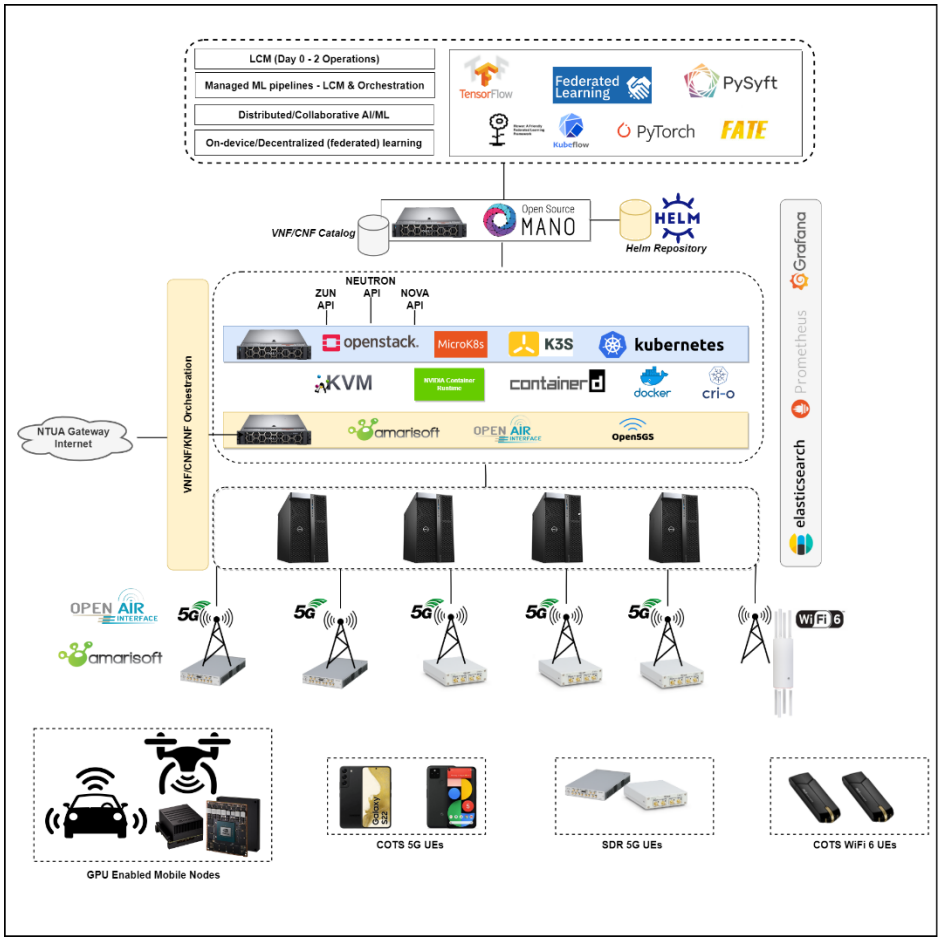

Figure 34: 5G Testbed at ICCS

Experimentation at ICCS lab facilities will exploit Module 2 and Module-4 to perform various tests with respect to network KPIs including latency, throughput, jitter, network reliability (packet loss) and availability. The tests will be facilitated mainly by the *iperf* tool (an open-source software tool that is used to measure the network performance metrics), and *ping* to test the reachability of a host, and measure the round-trip time it takes for a packet of data to travel from the source to the destination and back. Module-2 will be integrated with the 10G NICs provided by NVIDIA for the generation and reception of real time traffic. The performance of the end-to-end system will be tested while utilizing passive cyclic arrayed waveguide gratings (cAWGs) an all-optical packet switching network will be implemented and tested. Additionally, regarding Module-4 for the FSO link Module-4 will be connected with 10G NICs[1] and for the mmWave operation with the BB/IFU establishing wireless connectivity.

Then Module 2/Module-4 will be connected to ICCS host devices at NTUA campus for performing all relevant experimentation. Test KPIs are defined in Table 2.

[1] 10G NICs are the same described in 3.2 programmed to operate with only one lane working at 10G/s

Table 2: Module-2/-4 end to end testing: KPIs

KPI ID	KPI1
KPI	End-to-End Latency.
Description	Measured round-trip-time (RTT) from the moment the IP ICMP Echo Request packet leaves the source host until the IP ICMP Echo Reply is received from the destination host.
Data Needed	Time from Source to Target Device (i.e. measured at the communication interface).
Owner	ICCS

KPI ID	KPI2
KPI	Reliability
Description	The percentage (%) of the amount of sent network layer packets successfully delivered to a given system node divided by the total number of sent network layer packets.
Data Needed	Packets Successfully Delivered, Total Number of Packets.
Owner	ICCS

KPI ID	KPI3
KPI	Availability
Description	Percentage of successful connection tests (RTT) to the reference service endpoint over a period of time between ICCS hosts connected to module 2/4.
Data Needed	Time Delivering, Total Time of Observation
Owner	ICCS

KPI ID	KPI4
KPI	Bandwidth
Description	Maximum TCP/IP uplink and downlink bandwidth measured between the ICCS hosts connected to module 2/4.
Data Needed	Time Delivering, Total Time of Observation
Owner	ICCS

KPI ID	KPI5
KPI	Packet delay variation
Description	The variation in the delay of received packets between ICCS hosts connected to module 2/4
Data Needed	Timestamp at packet transmission, timestamp at packet reception
Owner	ICCS

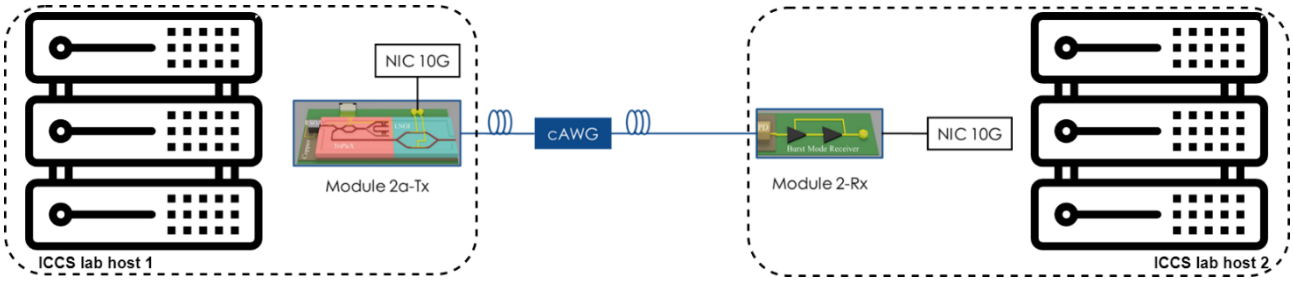

Figure 35: Module-2 end to end testing.

In Figure 36 the diverse links that will be tested employing Module-4 are presented.

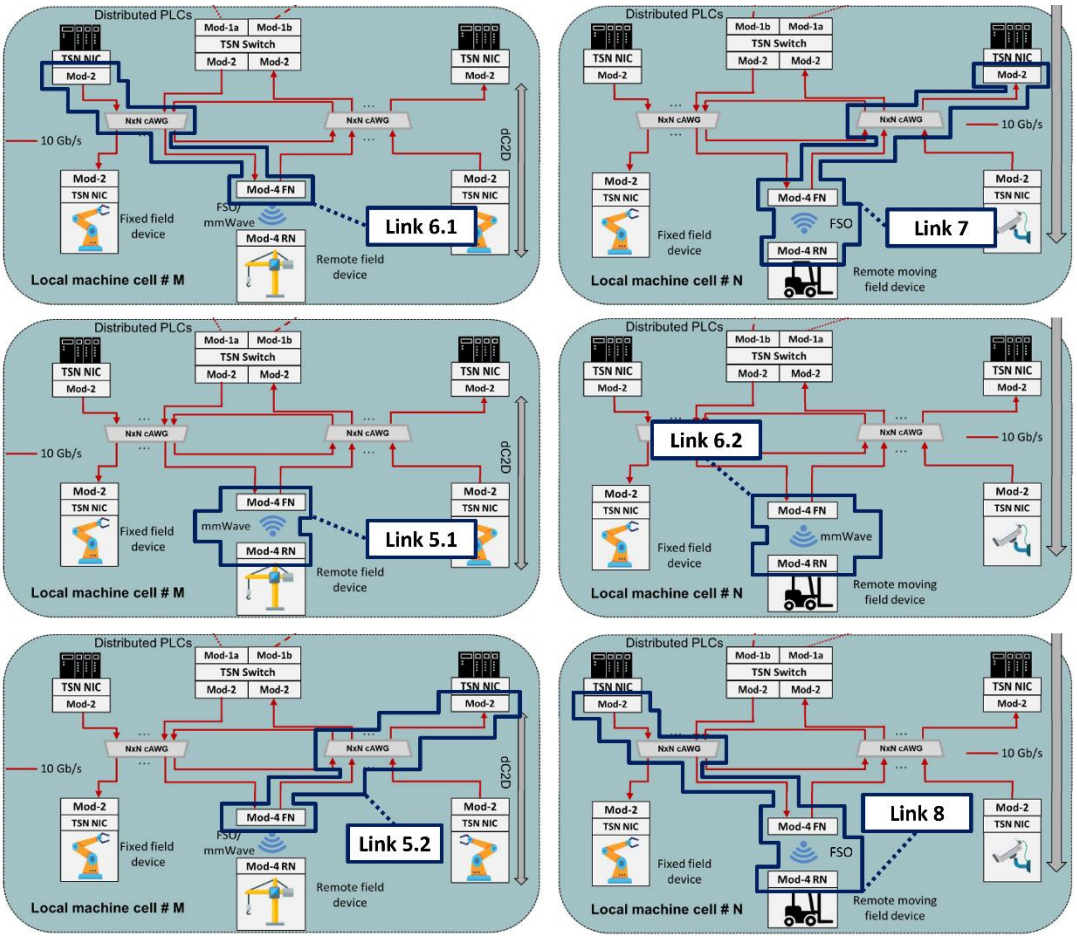

Figure 36: Module-4 link topologies.

4 INDUSTRIAL PREMISES FIELD TRIAL

Chapter 4 is intended to describe the application of technologies developed within SPRINTER project in a factory premise, where it is possible to demonstrate the potentialities mobilized by a powerful and ubiquitous connectivity.

The aim of the field trials is to test the application performances relating them to network ones and their optical and wireless connectivity. More specifically, the application should reach the theoretical maximum bandwidth resulting from the allocation of optical connections at any given time.

4.1 FILL factory field trial

To verify the SPRINTER technology in a field test, two distinct test setups (details in section 4.1.1 and 4.1.2) were devised. These setups show different application scenarios of SPRINTER technology in modern production industry and show the potential and possibilities of SPRINTER technology.

For each of the two setups, three different applications will be implemented. The first involves the geometric calibration of the robot (further details in section 4.1.3), the second is a high-precision trajectory tracking control (section 4.1.4). The key aspect of both applications is the detection of the robot's end-effector pose using cameras, as described in section 4.1.5. In a third test application, the camera-based pose detection is validated with a laser tracker system.

4.1.1 Field Trial Setup 1 (Direct Connection)

The first test setup (illustrated in Figure 37) demonstrates the application of SPRINTER technology, where multiple end devices (in this case, high-speed, high-resolution cameras) are connected via SPRINTER technology to a computing unit for further data processing.

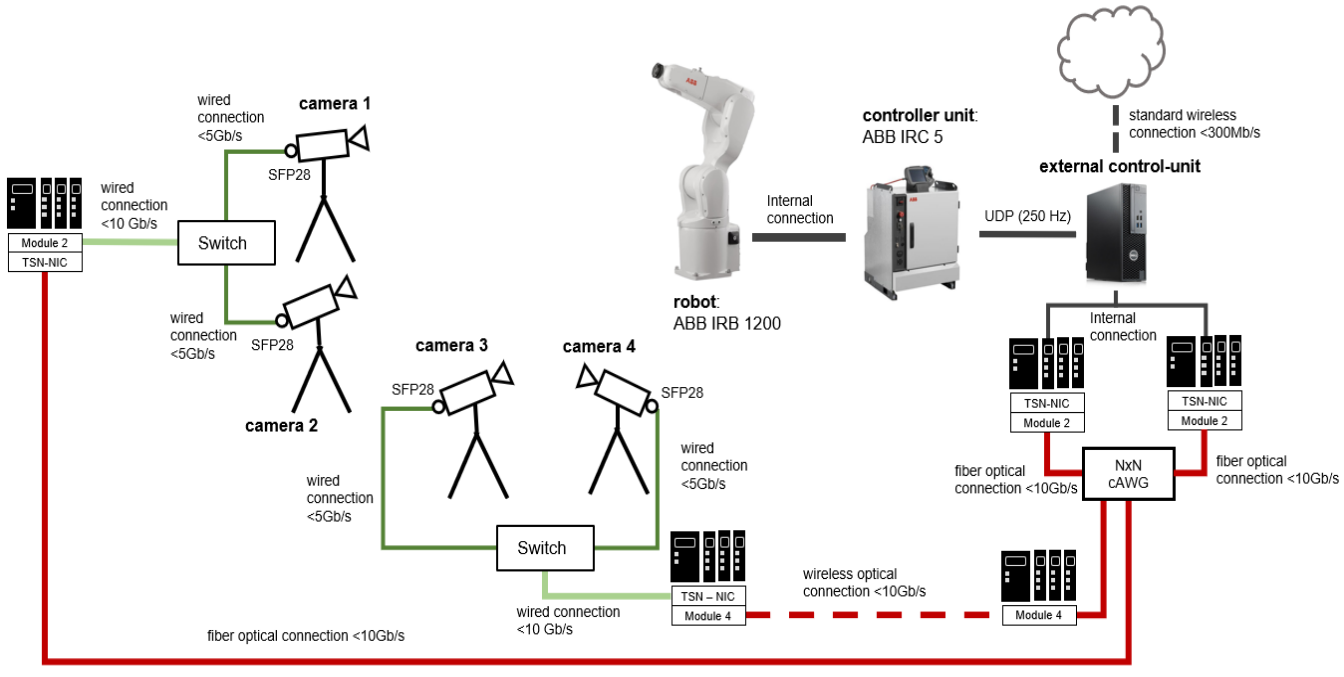

Figure 37: Trial Setup 1

In detail, image data (indicated in dark green in Figure 37) from two cameras is streamed, with a data rate lower than 5 Gbit/s and is aggregated on a switch. The switch can be used to prioritize which camera image is most important based on the current position of the robot. The aggregated data, with a data rate lower than 10 Gbit/s (marked in light green in Figure 37), is transmitted through module 2 over a fibre-optical connection (indicated in dark red) to a cyclic Arrayed Waveguide Grating (cAWG). Similarly, the wireless connection from two additional cameras, using module 4, is set up to the same cAWG.

The cAWG connects the addressing of the receiver modules routing traffic to the port correspondent to the wavelength of the transmitter modules, simulating the industrial application of splitting the data stream between different computing units. The receiver modules are connected via network cards (Nvidia CONNECTX-6 DX cards) to the external computing unit, an industrial server specified to meet real-time control and image processing requirements, as well as network architecture.

Via Ethernet, the server communicates with the ABB IRC5 robot controller using a UDP protocol, reading the current joint angles every 4 milliseconds and sending movement commands. The ABB IRB 1200 industrial robot serves as the robot for these tests.

The robot, its controller, and the external control unit are mounted on a movable base plate, allowing flexibility in the setup's location. The cameras, mounted on tripods, and the entire setup occupy an approximate space of 6 x 6 meters. Initial tests will be conducted in the Fill Future Zone, a standard industrial environment.

Figure 37 represents components involved in test setup and their connectivity as a general overview. Precise identification of components is still ongoing, e.g. the camera types used for the demonstration could be changed to the most suitable for the end-effector identification described in 4.1.5.

Table 3: Hardware Components and Specifications for Trial Setup

Hardware components	Specifications
Robot	ABB IRB1200-7/0.7 Range: 703 mm, payload: 7 kg, number of joints: 6 Standard repeatability: 0,02 mm (not absolute motion accuracy!)
Robot Control unit	ABB IRC5 Single
IR-filtered Cameras	Emergent Vision BOLT-Series Model: HB-9000-G-M Pixel: 4200 x 2160 BPP: 8/10 bits fps: 290 Interface: 25GigE SFP28
Lens	Kowa LM12FC24M focual length: 12mm
IR-Filter	MidOpt LP830 – 35.5
Focus tunable lense	Optotune EL-16-40-TC-NIR-5D-C
Lasertracker	Leica AT960 Accuracy: 0.025mm
Computer/Server	Not specified yet
TSN - NICs	NVIDIA CONNECTX-6 DX PCIe x16 HHHL Card Maximum total bandwidth: 200 Gb/s Number of network ports: 2

4.1.2 Field Trial Setup 2 (Industrial Network)

The second test setup (shown in Figure 38) illustrates the application of SPRINTER technology, where multiple devices communicate via a 100 Gb/s (4x25Gb/s) fibre optical TSN backbone ring defined on SPRINTER architecture with a server. Each device includes several sensors, also connected with

SPRINTER technology, with the sensors being high-speed, high-resolution cameras and the devices being TSN-Switches.

In detail, the image data from the four cameras is streamed with a data rate below 10 Gb/s. Each camera is individually connected (marked in green in Figure 38) to SPRINTER modules 2 or 4 via a TSN NIC. The SPRINTER modules establish connections to the TSN-Switch, with control over addressing the receiver module through an cAWG. These TSN switches are not physical switches but are simulated by the server and the NICs, where a program on the server performs switch operations on the ports.

Furthermore, the switches are connected with Module 1 to the TSN backbone.

The TSN backbone (marked in blue) is simulated using different ports of the server, with each port having a Nvidia CONNECTX-6 DX card connected to the module 1. The reason for this setup in SPRINTER is to achieve the time schedule for network packet flows. So, whenever a specific permutation is imposed by the optical switch on the network, the packets for the right destinations are on the wires. This avoids congestion on the network and allows communication with minimum jitter. Moreover, TSN NIC driver features forwarding support to schedule traffic towards different destinations when multiple NICs are used in the same server. This additional forwarding action for each time schedule is provided by the SPRINTER Control plane.

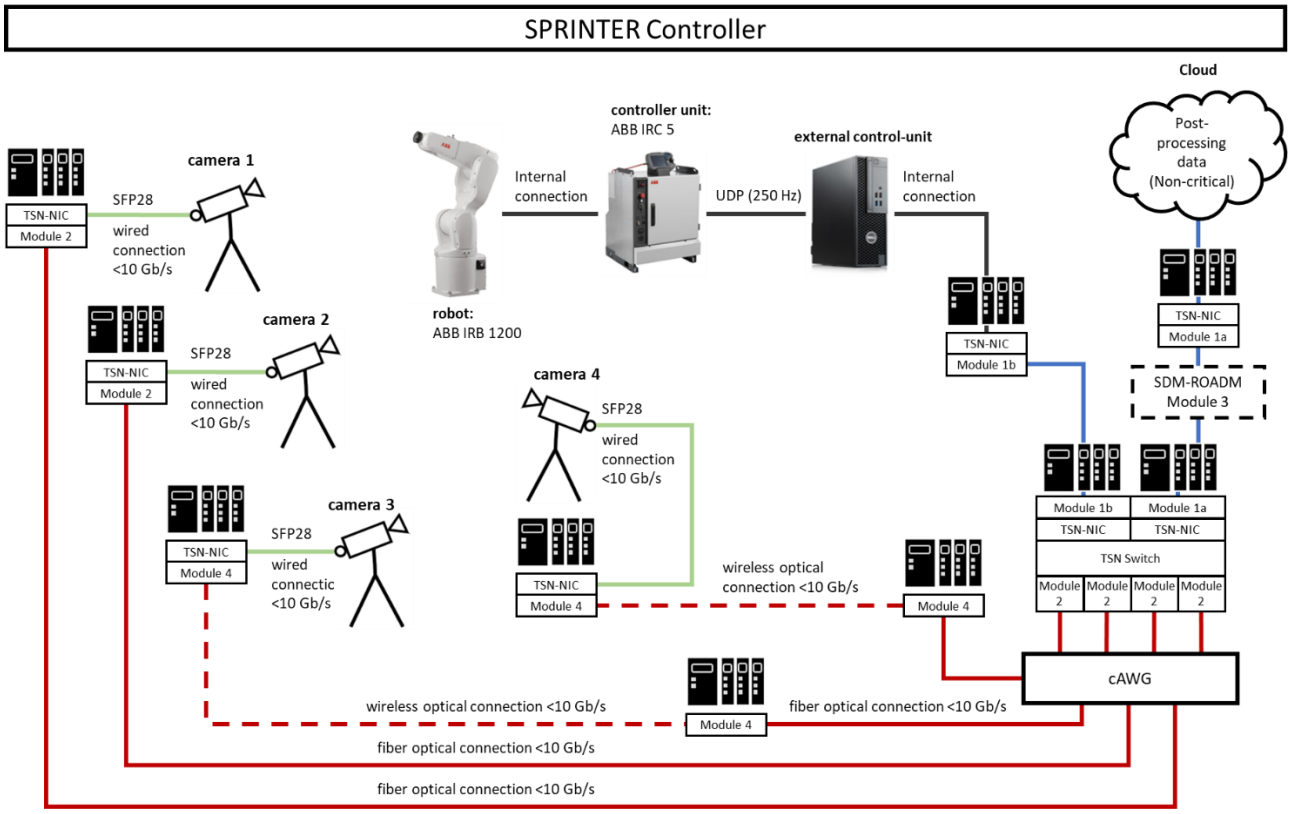

Figure 38: Test Setup 2

Similar to Trial Setup 1 (section 4.1.1), the robot, its controller, and the external control unit are mounted on a movable base plate. The cameras will be mounted on tripods and the entire setup will occupy an approximate space of 6 x 6 meters for initial tests in the Fill Future Zone in industrial environment.

Details of the setup are provided in Figure 38 where connectivity towards external control units are realized in accordance with general SPRINTER network architecture described in [1].

4.1.3 Test Application 1 (Geometric Calibration)

In the geometric calibration, precision is crucial for determining the pose with high accuracy. Image data, captured at very high resolution, results in large amounts of data, but the speed of data transmission is less critical as the end-effector pose doesn't require real-time calculation.

The end-effector poses from the images are used to determine the geometric parameters of the robot in an algorithm running offline on the external control unit. These parameters are then adopted

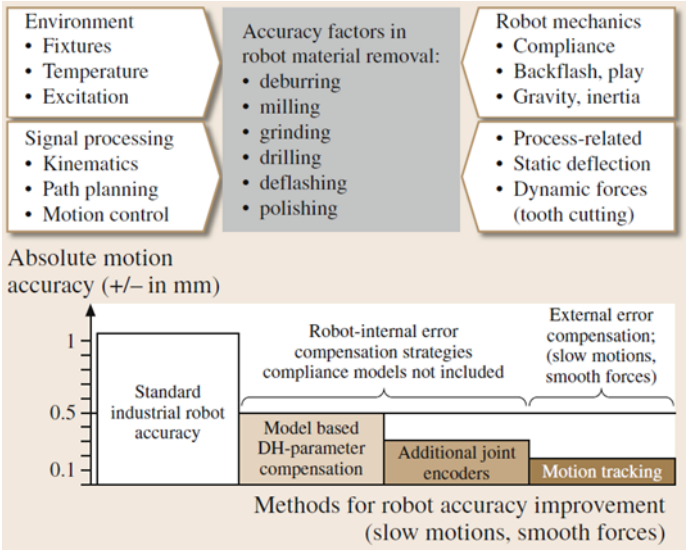

Figure 39: Influences on Positional Accuracy of IR and Methods to Increase

in the robot controller, enhancing positional accuracy to an expected range of 0.5 mm (refer to Figure 39). Additional details about the end-effector detection in section 4.1.5.

To test SPRINTER technology, geometric calibration will be executed with different test settings, as detailed in section 4.1.6. These settings vary in data rate, set via the framerate and the resolution of the camera. (Not all settings described in section 4.1.6. are relevant.)

4.1.4 Test Application 2 (High-precision Trajectory Tracking Control)

In high-precision control, speed and low latency of image data transmission are essential. The latency time and transmission reliability significantly impact the control loop's cycle time, requiring sensor data to be transmitted faster than this cycle time for effective data processing.

The high-precision control involves transmitting camera data to the external control unit at high speed. The current end-effector pose is determined from this data (refer to section 4.1.5 for details), and a control value is derived using a control law, sent from the external control unit to the robot controller. The robot controller then executes motor control to move the robot to the new corrected target position. The objective is to achieve improved accuracy within the range of 0.2 mm, as depicted in Figure 39. The achievable accuracy depends on the end-effector pose determination accuracy and the transmission cycle time.

As in the section before the application will be executed with different test settings, as detailed in section 4.1.6. These settings vary in data rate, set via the framerate and the resolution of the camera. (Not all settings described in section 4.1.6. are relevant.)

4.1.5 Test Application 3 (Detection of the Robot's End-Effector Pose)

End-effector pose detection involves attaching a marker with infrared reflectors to the robot's end-effector. Four cameras with infrared filters record the working area, and a processor on each camera determines the area where reflectors should be located, transmitting sub-frames to the external computing unit.

The external computing unit calculates the position of the reflectors in the sub-images, determining the end-effector pose in world coordinates. This information is used for geometric calibration (section 454.1.3) or high-precision control (section 4.1.4.). A laser tracker attached to the end-effector

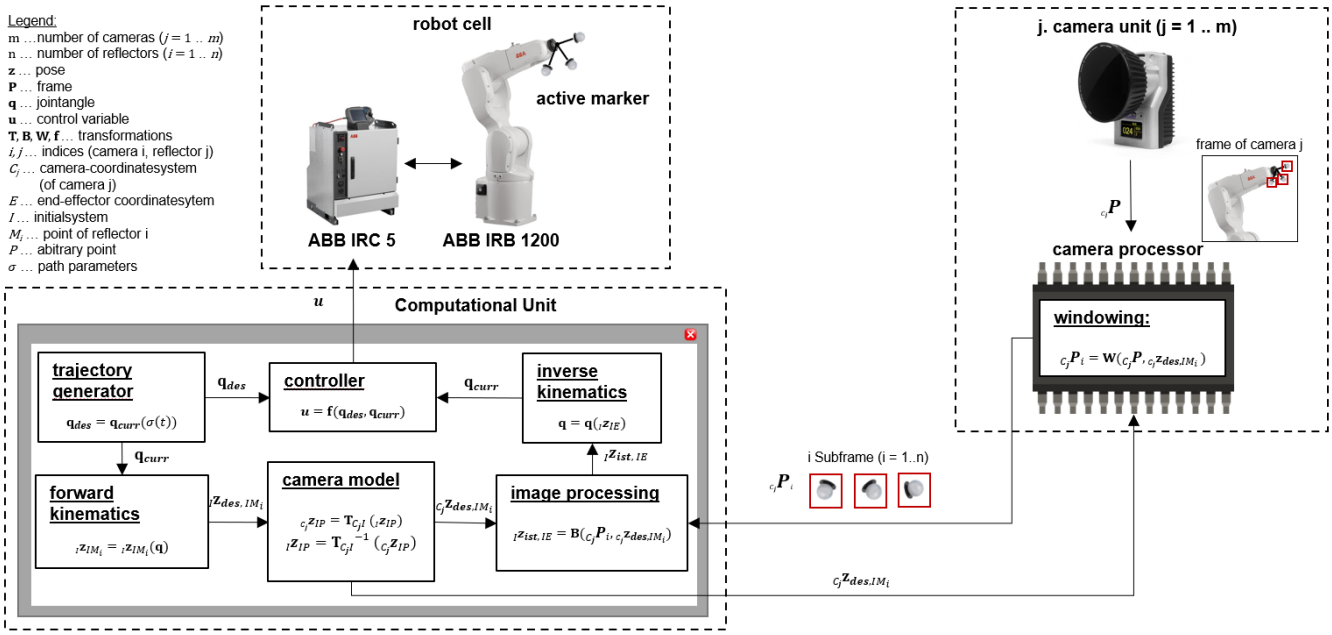

Figure 40: Concept of EE-Detection

provides an additional method to verify the camera-based system's end-effector pose determination.

A sketch of the whole process can be seen in Figure 40, the different Camera settings are described in section 4.1.6.

4.1.6 Test Settings

The accuracy of EE detection depends on various factors, including environmental influences, quality of IR illumination, and the number of cameras, their resolution, and the number of reflectors on the marker.

Neglecting the environmental influences results in a theoretical maximum achievable accuracy depending on the number of cameras, the camera resolution and the number and size of the reflectors. The camera resolution (Res_{Area}) and the frame rate (R_{frame}) determine how high the required data rate (R_{data}) of the SPRINTER modules must be. This is calculated via Equation (1), where R_{data} is the data rate, Res_{Area} the total resolution ($Res_{Area} = Res_x \cdot Res_y$), R_{frame} the framerate, cS the channel size, pD the pixel Depth and F_{comp} a compression factor.

$$R_{data} = Res_{Area} \cdot R_{frame} \cdot cS \cdot pD \cdot F_{comp} \quad (1)$$

As the data rate of the modules is limited to 10 Gb/s but the selected camera would manage 20 Gb/s, there is a trade-off between resolution and frame rate, because of this reason, various test scenarios were defined for testing the modules, which can be seen in Table 4: Test Scenarios.

These test cases differ in the maximum accuracy of EE detection (acc_{max}) as well as in the latency of data transmission and show which data rates are to be expected on the SPRINTER Modules. The maximum accuracy is related to the resolution of the camera and is calculated according to Equation (2) and the latency is the inverse of the framerate. For maximum accuracy of EE detection, the resolution of the camera is varied between 2 and 9 MP and for the latency the framerate of the camera is varied between 4 ms to 20 ms.

$$acc_{max} = \max\left(\frac{Res_x}{x}, \frac{Res_y}{y}\right) \cdot \frac{d-f}{f} \cdot F_{acc} \quad (2)$$

The table also shows the maximum properties of the camera. However, it should be noted that in this line, the accuracy of the camera is that which a camera without sub-pixel technology can theoretically achieve.

Table 4: Test Scenarios

scenario	camera	resolution	data-rate	accuracy of marker detection	latency
MoCap sytem	Oqus 6+	3072x1984	0,1 Gbps	1 mm	2,2 ms
maximum	HB-9000-G-M	4200x2160	21,0 Gbps	0,62 mm	3,4 ms
test setting 1	HB-9000-G-M	1972x1014	0,8 Gbps	0,27 mm	20 ms
test setting 2	HB-9000-G-M	1972x1014	4,0 Gbps	0,27 mm	4 ms
test setting 3	HB-9000-G-M	2415x1242	6,0 Gbps	0,22 mm	4 ms
test setting 4	HB-9000-G-M	3416x1757	4,8 Gbps	0,15 mm	10 ms
test setting 5	HB-9000-G-M	4200x2160	7,3 Gbps	0,12 mm	10 ms
test setting 6	HB-9000-G-M	4200x2160	10,2 Gbps	0,12 mm	7 ms

For comparison, the table shows the data of a motion capturing system that is already on the market. In this system, however, the marker positions are calculated directly at the camera and only these are transmitted, resulting in very low data rates, with the disadvantage that the camera images cannot be used any further. All values here are the actual values of the system and not theoretical estimates.

The test cases in Table 4 are roughly categorized into well-functioning/desired requirement (marked in green), close to functionality threshold/to be verified (marked in orange) and beyond functionality threshold/out of spec (marked in red).

As it can be seen in the line with the maximum properties of a camera, a data rate of 21Gbps is achieved when operating the camera with maximum properties, but this data rate would far exceed the requirements for modules 2 and 4 of SPRINTER technology. For this reason, there is a trade-off between maximum resolution (setting 6) (equally important with max accuracy) and maximum transmission speed (setting 3). In the other settings, these values were varied so that different levels for the data rate are achieved for testing the SPRINTER technology.

5 CONCLUSIONS

This deliverable is the outcome of the initial activities carried out in the framework of WP7. It represents the output of *T7.1-Definition of testing procedures and demonstration scenarios* and uses the work done in optical and network component definition, specification and KPIs identification within WP2 and WP6 to design testing setups and methodologies suitable to validate SPRINTER prototypes with reference to KPIs presented in *D2.1 - Definition of application scenarios, system requirements and specifications at the network, module, and component level [1]*.

The chosen approach is to have, for each optical or network component developed within the project, a testing strategy organized in three phases: module level, system level and industrial application level; each test phase is capable to capture and validate different characteristics of SPRINTER prototypes and to assess their capability to interoperate to realize SPRINTER's innovative architecture.

The phased approach to prototypes validation makes possible an early discovery and fixing of potential non-compliances minimizing the project risk.

To each test phase is assigned a different chapter inside this deliverable and activities described there will be executed and documented within the following tasks of WP7:

- D7.1 Chapter 2
  - T7.2-System integration of SPRINTER prototypes
  - T7.3-Performance validation of SPRINTER prototypes in lab settings
- D7.1 Chapter 3
  - T7.4-Performance evaluation of SPRINTER prototypes in TSN-enabled infrastructure
- D7.1 Chapter 4
  - T7.5-Demonstration of SPRINTER technology in a relevant industrial environment

For this reason, this deliverable, forms the foundation for the development of SPRINTER technology demonstrators and will guide the activities inside *WP7- System integration and testing of SPRINTER prototypes* till the completion of the project.

List of Figures

List of Tables

References

[1] D2.1 - Definition of application scenarios, system requirements and specifications at the network, module and component level.
[2] Openairinterface the fastest growing community and SW assets in 5G wireless, website, https://openairinterface.org/
[3] Amarisoft 4G-5G, website, https://www.amarisoft.com/
[4] Open 5GS Open Source implementation for 5G Core and EPC, website, https://open5gs.org/
[5] CPRI Common Public Radio Interface, website, http://www.cpri.info/
[6] NVIDIA CONNECTX-6 DX Ethernet SmartNIC, datasheet, https://www.nvidia.com/content/dam/en-zz/Solutions/networking/ethernet-adapters/connectX-6-dx-datasheet.pdf
[7] PCIe slot for CONNECTX-6 specification, webpage, https://docs.nvidia.com/networking/display/connectx6vpi/specifications#src-94799462_Specifications-MCX683105AN-HDATSpecifications
[8] QSFP28 to SFP28 adapter, datasheet, https://network.nvidia.com/related-docs/prod_cables/PB_QSA28.pdf
[9] Ericsson 5G RAN – Radio Access Network, webpage, https://www.ericsson.com/en/ran